

Joint estimation of asymmetric community numbers in directed networks

Huan Qing^{a,*}

^a*School of Economics and Finance, Chongqing University of Technology, Chongqing, 400054, China*

Abstract

Community detection in directed networks is a central task in network analysis. Unlike undirected networks, directed networks encode inherently asymmetric relationships, giving rise to sender and receiver roles that may each follow distinct community organizations with possibly different numbers of communities. Estimating these two community counts simultaneously is therefore considerably more challenging than in the undirected setting, yet it is essential for faithful model specification and reliable downstream inference. This work addresses this challenge within the stochastic co-block model (ScBM), a powerful statistical framework for capturing asymmetric relational structures inherent in directed networks. We propose a novel goodness-of-fit test based on the deviation of the largest singular value of a normalized residual matrix from the constant value 2. We show that the upper bound of this test statistic converges to zero under the null hypothesis, while this statistic goes to infinity if the true model has finer communities than hypothesized. Leveraging this tail bounds behavior, we develop an efficient sequential testing algorithm that lexicographically explores candidate community number pairs. To enhance robustness in practical settings, we further introduce a ratio-based variant that detects the transition point in the test statistic sequence. We rigorously show both algorithms' consistency in recovering the true sender and receiver community counts under ScBM. Numerical experiments demonstrate the accuracy and robustness of our methods in estimating community numbers across diverse ScBM settings.

Keywords: Goodness-of-fit test, ScBM, Directed networks, Community detection, Singular value tail bounds

1. Introduction

Directed networks are ubiquitous in real-world complex systems, capturing asymmetric relationships where interactions exhibit inherent directionality [25]. For example, in social media platforms like Twitter, users follow one another directionally, creating a directed network of influence. In email exchanges, senders send emails to receivers,

*Corresponding author.

Email address: qinghuan@cqut.edu.cn&qinghuan@u.nus.edu (Huan Qing)

creating send-to relationships [30]. In academic citation networks, papers cite others without reciprocal acknowledgment, forming a directed structure of knowledge flow [13, 14]. These examples illustrate that directed networks encode edge relationships with distinct “sender” (edge origins) and “receiver” (edge destinations) roles, fundamentally different from undirected networks where connections are symmetric [30]. The study of such asymmetric relational patterns is critical for understanding complex systems, as the directionality often encodes functional or causal dependencies.

Community detection in directed networks aims to identify groups of nodes with similar interaction patterns, distinguishing between sender-based and receiver-based communities [21, 25, 30]. This task is crucial for applications such as identifying opinion leaders in social networks, mapping intellectual communities in citation graphs, optimizing traffic routing in transportation systems, and market segments in stock networks [22]. Unlike undirected networks, where communities imply symmetric associations, directionality of directed networks introduces unique challenges: sender communities (nodes with similar outgoing edge patterns) and receiver communities (nodes with similar incoming edge patterns) may exhibit distinct organizational structures, including potentially different numbers of communities [30]. Faithfully recovering these asymmetric structures is essential for learning complex structures in directed networks.

The stochastic co-block model (ScBM) proposed in [30] is a powerful statistical framework for modeling directed networks with asymmetric community structure. It extends the classical stochastic block model (SBM) [9] from undirected networks to directed networks by introducing dual community memberships: each node belongs to a sender community governing its outgoing edges and to a receiver community influencing its incoming edges. Formally, ScBM assumes that each node belongs to a sender community and a receiver community, and the probability of an edge from node i to node j depends on the sender community of i and the receiver community of j . This dual assignment mechanism enables ScBM to capture the inherent directionality of relationships while accommodating potential asymmetry between sending and receiving behaviors. ScBM is particularly powerful for capturing scenarios where the number of sender communities differs from that of receiver communities. Numerous community detection methods have been developed for ScBM, including various spectral clustering approaches [30, 39, 35, 29, 8] and variational inference algorithms [40, 38]. However, all these existing methods require that both sender community count K_s and receiver community count K_r are known in advance, which is a significant practical limitation since the numbers of sender and receiver communities in real-world directed networks are rarely known. This limitation necessitates reliable joint estimation of both community numbers before meaningful community detection can proceed.

In undirected networks, community number estimation under SBM or its degree-corrected extension [16] has been addressed through various techniques including likelihood ratio tests [34, 24], Bayesian information criterion [26, 31],

[10], network cross-validation [3, 23], spectrum of the Bethe Hessian matrices [18, 12], and goodness-of-fit tests [2, 19, 5, 11, 15, 36]. However, these approaches fail in directed settings due to the dual community assignment mechanism of ScBM, where the number of sender communities may even be different from that of receiver communities. To our knowledge, no existing method provides theoretically guaranteed joint estimation of (K_s, K_r) for directed networks under ScBM. This paper bridges the gap by developing a framework for jointly estimating the numbers of sender and receiver communities within the ScBM framework. Our key contributions are threefold:

- We propose a novel test statistic based on the deviation of the largest singular value of a normalized residual matrix from the constant 2. This test statistic leverages the tail behavior of singular values rather than their asymptotic distribution—a crucial innovation necessitated by the asymmetric nature of directed networks.
- We establish rigorous theoretical guarantees to show that under correct model specification, the test statistic’s upper bound converges to zero with high probability, while under underfitted models, the statistic diverges to infinity. This dichotomous behavior provides a statistical foundation for model selection in directed networks.
- We propose two computationally efficient algorithms: a sequential testing procedure that lexicographically explores candidate asymmetric community number pairs using a decaying threshold, and a ratio-based variant that detects the transition point in the test statistic sequence for enhanced robustness in practical settings. We prove the consistency of both estimators under ScBM with mild conditions and conduct extensive numerical experiments to validate their accuracy across diverse ScBM configurations, demonstrating robustness to threshold selection and applicability to real-world directed networks.

2. Model formulation and problem statement

This section formally defines the Stochastic co-block model (ScBM) and precisely states the core estimation problem. We specify the ScBM’s generative mechanism, which incorporates distinct sender and receiver community memberships to model asymmetric edge directionality. The central problem addressed is the joint estimation of the unknown sender and receiver community counts (K_s, K_r) from observed network data. Necessary theoretical assumptions for establishing theoretical guarantees are also presented.

2.1. Stochastic co-block model (ScBM)

In this paper, we study a directed network on n vertices represented by an adjacency matrix $A \in \{0, 1\}^{n \times n}$, where $A_{ii} = 0$ and $A_{ij} = 1$ signifies a directed edge sending from node i to node j . The *stochastic co-block model* (ScBM) partitions the n vertices into K_s *sender communities* and K_r *receiver communities* [30]. Formally, the model is specified as follows:

Definition 1 (Stochastic co-block model (ScBM)). *Consider a directed network with n nodes. Let $A \in \{0, 1\}^{n \times n}$ be the adjacency matrix where $A_{ii} = 0$ and $A_{ij} = 1$ indicates a directed edge from node i to node j . The stochastic co-block model (ScBM) is parameterized by:*

- *Sender community labels: $g^s \in \{1, \dots, K_s\}^n$.*
- *Receiver community labels: $g^r \in \{1, \dots, K_r\}^n$.*
- *Block probability matrix: $B \in [0, 1]^{K_s \times K_r}$.*

Given (g^s, g^r, B) , the entries of A are independent with

$$\mathbb{P}(A(i, j) = 1) = B(g^s(i), g^r(j)), \quad \forall i \neq j.$$

The expected adjacency matrix Ω satisfies $\Omega(i, j) = B(g^s(i), g^r(j))$ for $i \neq j$ and $\Omega(i, i) = 0$.

Sure, the sender-receiver asymmetry allows $g^s \neq g^r$ and $K_s \neq K_r$, enabling flexible modeling of asymmetric relational patterns in directed networks.

2.2. Core problem: joint community number estimation

In this paper, we address the fundamental problem of *community number estimation* in ScBMs: given a directed network, how can we jointly determine the numbers of sender communities K_s and receiver communities K_r ? We formulate this as a sequential goodness-of-fit testing problem: for candidate pairs (K_{s0}, K_{r0}) , we test

$$H_0 : (K_s, K_r) = (K_{s0}, K_{r0}) \quad \text{versus} \quad H_1 : K_s > K_{s0} \text{ or } K_r > K_{r0},$$

where H_1 explicitly encodes *underfitting* scenarios where the hypothesized model lacks sufficient sender or receiver communities. This formulation is statistically challenging and practically significant for three reasons:

1. The bivariate community structure (K_s, K_r) creates a combinatorial search space of size $(K_s + K_r)^2$, requiring efficient testing strategies.
2. Underfitting (failing to reject H_0 when H_1 holds) leads to loss of structural resolution, while overfitting is mitigated algorithmically via ordered search.
3. Existing goodness-of-fit tests for undirected networks rely on symmetric eigenvalue distributions (e.g., Tracy-Widom laws analyzed in [19]) that do not extend to the asymmetric singular value decompositions required for directed networks.

Given that few existing methods provide theoretically guaranteed joint estimation of (K_s, K_r) in ScBM for directed networks, this work bridges this gap by developing a testing framework based on singular value tail bounds of normalized residual matrices. Our approach leverages the asymptotic behavior of the largest singular value under H_0 versus H_1 , enabling consistent community number estimation.

2.3. Theoretical assumptions

To establish theoretical guarantees, we require the following regularity conditions:

Assumption 1 (Bounded edge probabilities). *The block probability matrix satisfies $\delta \leq B(k, l) \leq 1 - \delta$ for all k, l and some $\delta > 0$.*

Assumption 1 ensures well-defined variance in the residual matrix defined later and excludes degenerate cases where normalization becomes unstable.

Assumption 2 (Balanced community sizes). *The community sizes satisfy:*

$$\min_{k=1, \dots, K_s} |\{i : g^s(i) = k\}| \geq c_0 \frac{n}{K_s}, \quad \min_{l=1, \dots, K_r} |\{j : g^r(j) = l\}| \geq c_0 \frac{n}{K_r}$$

for some $c_0 > 0$.

Assumption 2 prevents any community from being asymptotically negligible, guaranteeing that the sample size within every block grows linearly with n . Similar assumptions are also required for theoretical guarantees of goodness-of-fit test in undirected networks under SBM [19, 11, 36, 37]

Define $K_{\max} = \max(K_s, K_r)$ and the community separation metric:

$$\delta_n = \min \left(\min_{k \neq k'} \max_l |B(k, l) - B(k', l)|, \min_{l \neq l'} \max_k |B(k, l) - B(k, l')| \right).$$

The community separation δ_n quantifies the minimal distinguishability between communities through capturing the worst-case discriminability between any two sender or receiver communities.

Assumption 3 (Model complexity and community distinguishability).

$$\frac{K_{\max}^2 \max(\log n, \delta_n^{-2})}{n} \rightarrow 0 \quad \text{as} \quad n \rightarrow \infty,$$

which also implies: (1) $K_{\max} \ll \sqrt{n/\log n}$ limiting model complexity; (2) $\delta_n \gg n^{-1/2}$ ensuring communities are statistically distinguishable.

Assumption 3 establishes a fundamental trade-off between model complexity captured by K_{\max} and community separability described by δ_n that ensures the asymptotic controllability of the test statistic. Further understandings of Assumption 3 are provided in the following remark.

Remark 1. The condition $\frac{K_{\max}^2 \max(\log n, \delta_n^{-2})}{n} \rightarrow 0$ adaptively constrains the interplay between model complexity and community separability depending on the relative scaling of δ_n and n , which we analyze through two typical regimes:

Case 1: $\delta_n^{-2} \geq \log n$ (weak separation). Here $\max(\log n, \delta_n^{-2}) = \delta_n^{-2}$, reducing the assumption to $\frac{K_{\max}^2}{n\delta_n^2} \rightarrow 0$. This yields the sandwich bound

$$\frac{K_{\max}}{\sqrt{n}} \ll \delta_n \leq \frac{1}{\sqrt{\log n}}.$$

The sandwich bound explicitly balances separation and complexity: models with larger K_{\max} require stronger separation (larger δ_n), while weaker community separation (smaller δ_n) requires fewer communities. Meanwhile, the minimal separation must dominate the parametric rate K_{\max}/\sqrt{n} . For fixed K_{\max} , δ_n must decay slower than $n^{-1/2}$. If $K_{\max} \rightarrow \infty$ slowly (e.g., $K_{\max} = O(\log n)$), δ_n must decay slower than $\log n/\sqrt{n}$.

Case 2: $\delta_n^{-2} < \log n$ (strong separation). Here $\max(\log n, \delta_n^{-2}) = \log n$, simplifying the assumption to $\frac{K_{\max}^2 \log n}{n} \rightarrow 0$, equivalent to $K_{\max} \ll \sqrt{n/\log n}$. In this regime, separation is relatively strong ($\delta_n > \frac{1}{\sqrt{\log n}}$), so community distinguishability is not the binding constraint. The assumption reduces to limiting model complexity: K_{\max} must grow slower than $\sqrt{n/\log n}$. For fixed K_{\max} , the condition holds trivially as $n \rightarrow \infty$.

3. Goodness-of-fit test

This section develops a theoretically grounded goodness-of-fit test for ScBM. We first introduce an ideal test statistic using oracle parameters, then derive its practical counterpart with estimated parameters, and finally establish its asymptotic behavior under both null and alternative hypotheses. The core innovation lies in leveraging singular value tail bounds of normalized residual matrices to detect community underfitting.

3.1. Ideal test statistic and its asymptotic behavior

To formalize the test, we begin with the *ideal residual matrix* R constructed using true parameters:

$$R(i, j) = \begin{cases} \frac{A(i, j) - \Omega(i, j)}{\sqrt{(n-1)\Omega(i, j)(1-\Omega(i, j))}} & i \neq j, \\ 0 & i = j, \end{cases}$$

where $\Omega(i, j) = B(g^s(i), g^r(j))$ is the true edge probability. This normalization ensures $\mathbb{E}[R(i, j)] = 0$ and $\text{Var}(R(i, j)) = \frac{1}{n-1}$ for $i \neq j$, transforming R into a generalized random non-symmetric matrix with controlled variance. The ideal

test statistic is defined as:

$$T_n = \sigma_1(R) - 2, \quad (1)$$

where $\sigma_1(\cdot)$ denotes the largest singular value. The shift by 2 anticipates the asymptotic behavior of $\sigma_1(R)$ under H_0 , as established below.

Lemma 1. *Under H_0 and Assumption 1, for any $\epsilon > 0$, we have*

$$\mathbb{P}(T_n < \epsilon) \rightarrow 1 \quad \text{as } n \rightarrow \infty.$$

Proof intuition. The convergence follows from tail bounds for the largest singular value of random matrices with independent entries [1]. Specifically, Lemma 2 in the Appendix yields $\|R\| \leq 2(1 + \eta) + O_P(\sqrt{\log n/n})$ for any $\eta > 0$. The boundedness of $\Omega(i, j)$ guaranteed by Assumption 1 controls R 's variance. \square

Remark 2. *A crucial distinction arises when comparing to undirected networks: while [19] leveraged Tracy-Widom distributions for symmetric adjacency matrices, asymptotic distributions for directed residuals remain an open problem. This theoretical gap originates from the inherent asymmetry of the ideal residual matrix R in directed networks. Therefore, to rigorously determine the number of sender and receiver communities under the ScBM, we focus on characterizing the asymptotic behavior of our test statistic, rather than its asymptotic distribution.*

3.2. Test statistic and its asymptotic behavior

In the construction of the ideal test statistic T_n , we have used unknown model parameters (B, g^s, g^r) for real directed networks. Thus, T_n can not be used as a practical test statistic for real data. Next, we introduce an approximation of T_n by estimating the block probability matrix B and community labels g^s and g^r from the adjacency matrix A of a real directed network.

Let \mathcal{M} be any community detection algorithm for directed networks. Apply \mathcal{M} to A to partition the n nodes into K_{s0} *sender communities* and K_{r0} *receiver communities*, yielding estimated labels \hat{g}^s for sender community and \hat{g}^r for receiver community. Then, we compute B 's plug-in estimator $\hat{B} \in [0, 1]^{K_{s0} \times K_{r0}}$ via

$$\hat{B}(k, l) = \frac{\sum_{i: \hat{g}^s(i)=k} \sum_{j: \hat{g}^r(j)=l} A(i, j)}{|\{i : \hat{g}^s(i) = k\}| \cdot |\{j : \hat{g}^r(j) = l\}|}, \quad k = 1, \dots, K_{s0}, l = 1, \dots, K_{r0}.$$

From \hat{B} 's construction, we see that \hat{B} naturally extends the estimated block probability matrix used in [19] from undirected networks to directed networks.

The estimated expected adjacency matrix $\hat{\Omega}$ has entries $\hat{\Omega}(i, j) = \hat{B}(\hat{g}^s(i), \hat{g}^r(j))$ for $i \neq j$ and $\hat{\Omega}(i, i) = 0$. Then we construct the normalized residual matrix $\hat{R} \in \mathbb{R}^{n \times n}$ as

$$\hat{R}(i, j) = \begin{cases} \frac{A(i, j) - \hat{\Omega}(i, j)}{\sqrt{(n-1)\hat{\Omega}(i, j)(1-\hat{\Omega}(i, j))}} & i \neq j, \\ 0 & i = j. \end{cases} \quad (2)$$

When $(\hat{B}, \hat{g}^s, \hat{g}^r)$ are accurate enough under the null hypothesis $(K_s, K_r) = (K_{s0}, K_{r0})$, \hat{R} 's largest singular value should be a good estimation of $\sigma_1(R)$. Therefore, we use $\sigma_1(\hat{R})$ to define our practical test statistic as follows:

$$\hat{T}_n = \sigma_1(\hat{R}) - 2. \quad (3)$$

The normalization in \hat{R} ensures $\mathbb{E}[\hat{R}(i, j)] \approx 0$ and $\text{Var}[\hat{R}(i, j)] \approx (n-1)^{-1}$ under H_0 . The shift by 2 anticipates the asymptotic behavior of $\sigma_1(\hat{R})$'s upper bound under a correctly specified model, where $\sigma_1(\hat{R})$'s upper bound concentrates near 2 as shown by Theorem 1 given later. Under H_1 , $\sigma_1(\hat{R})$ diverges due to unmodeled community structure guaranteed by Theorem 2 given later.

While \mathcal{M} can be any method with consistent community recovery for directed networks under H_0 , this paper employs a simple spectral clustering approach for its theoretical guarantees and computational efficiency. Algorithm 1 details this procedure.

Algorithm 1 Spectral clustering for ScBM

Require: Adjacency matrix A , hypothesized community numbers pair (K_{s0}, K_{r0})

Ensure: Estimated labels \hat{g}^s, \hat{g}^r

- 1: Compute A 's truncated singular value decomposition: $A \approx U\Sigma V^\top$ where $U \in \mathbb{R}^{n \times K_{\min}}$, $V \in \mathbb{R}^{n \times K_{\min}}$, $U'U = I_{K_{\min} \times K_{\min}}$, $V'V = I_{K_{\min} \times K_{\min}}$, $K_{\min} = \min(K_{s0}, K_{r0})$, and $I_{K_{\min} \times K_{\min}}$ is a K_{\min} -by- K_{\min} identity matrix
- 2: Apply k -means with K_{s0} clusters to rows of U to obtain \hat{g}^s
- 3: Apply k -means with K_{r0} clusters to rows of V to obtain \hat{g}^r

This algorithm leverages the fact that, under ScBM, the singular vectors U and V encode the sender and receiver community structures, respectively [19]. The k -means step projects U and V into discrete labels, accommodating asymmetric sender-receiver roles. In fact, Algorithm 1 naturally extends the algorithm 1 studied in [20] from SBM to ScBM, and it is also the non-regularized and non-normalized version of the DI-SIM algorithm proposed in [30]. Its estimation consistency under ScBM can be found in [30, 29, 8].

Under H_0 , consistent estimation of communities ensures \hat{R} approximates R . We adopt [19]'s definition of consistency of community recovery.

Definition 2 (Consistency). \hat{g}^s and \hat{g}^r are consistent if $\mathbb{P}(\hat{g}^s = g^s) \rightarrow 1$ and $\mathbb{P}(\hat{g}^r = g^r) \rightarrow 1$ under H_0 .

Then, we have the following asymptotic result.

Theorem 1. Under H_0 and Assumptions 1-3, and let \hat{R} be obtained using consistent community estimators \hat{g}^s and \hat{g}^r , then for any $\epsilon > 0$, we have

$$\mathbb{P}(\hat{T}_n < \epsilon) \rightarrow 1 \quad \text{as } n \rightarrow \infty.$$

Theorem 1 guarantees that the upper bound of \hat{T}_n converges to 0 in probability under H_0 . This provides the theoretical basis for decision rules: small values of \hat{T}_n support H_0 , while large values signal model inadequacy. The following theorem guarantees that the test statistic diverges for underfitted models where $K_s > K_{s0}$ or $K_r > K_{r0}$.

Theorem 2. Under Assumptions 1-3, and if either $K_s > K_{s0}$ or $K_r > K_{r0}$ (or both), then

$$\hat{T}_n \xrightarrow{P} \infty.$$

This divergence property ensures that whenever the hypothesized model lacks sufficient sender or receiver communities, \hat{T}_n will exceed any fixed threshold with probability approaching 1. Combined with Theorem 1, this guarantees asymptotically separation between correctly specified and underfitted models.

4. Sequential estimation of community numbers

Building on the goodness-of-fit test developed in Section 3, we now address the core problem of joint community numbers estimation. The sequential testing framework leverages the asymptotic behavior of \hat{T}_n established in Theorems 1 and 2 to systematically identify the true (K_s, K_r) while maintaining computational efficiency. This approach transforms model selection into an ordered exploration of candidate pairs, where the test statistic's dichotomous behavior—convergence to zero under correct specification versus divergence under underfitting—provides reliable stopping criteria. We further propose a ratio-based variant of this approach to enhance robustness in practical settings.

4.1. Sequential testing algorithm and its estimation consistency

The estimation procedure evaluates candidate pairs (k_s, k_r) in *lexicographical order*:

$$(k_s, k_r) <_{\text{lex}} (k'_s, k'_r) \iff k_s + k_r < k'_s + k'_r \quad \text{or} \quad k_s + k_r = k'_s + k'_r \text{ and } k_s < k'_s.$$

This order prioritizes candidate pairs with smaller total community numbers $k_s + k_r$. Among pairs with the same total, those with a smaller sender community number k_s are prioritized. Let $\mathcal{P} = \{(k_s, k_r)\}_{m=1}^M$ be the lexicographically

ordered sequence of candidate pairs from $(1, 1)$ to (K_{\max}, K_{\max}) , where $M = K_{\max}^2$. The following example details of the lexicographical order of candidate pairs \mathcal{P} for $K_{\max} = 8$.

Example 1. Consider searching over candidate sender community numbers k_s from 1 to 8 and receiver community numbers k_r from 1 to 8. Table 1 provides the lexicographical order of candidate pairs \mathcal{P} for $K_{\max} = 8$.

Table 1: Lexicographical order of candidate pairs \mathcal{P} for $K_{\max} = 8$.

m	(k_s, k_r)												
1	(1,1)	9	(3,2)	17	(2,5)	25	(4,4)	33	(5,4)	41	(6,4)	49	(8,3)
2	(1,2)	10	(4,1)	18	(3,4)	26	(5,3)	34	(6,3)	42	(7,3)	50	(4,8)
3	(2,1)	11	(1,5)	19	(4,3)	27	(6,2)	35	(7,2)	43	(8,2)	51	(5,7)
4	(1,3)	12	(2,4)	20	(5,2)	28	(7,1)	36	(8,1)	44	(3,8)	52	(6,6)
5	(2,2)	13	(3,3)	21	(6,1)	29	(1,8)	37	(2,8)	45	(4,7)	53	(7,5)
6	(3,1)	14	(4,2)	22	(1,7)	30	(2,7)	38	(3,7)	46	(5,6)	54	(8,4)
7	(1,4)	15	(5,1)	23	(2,6)	31	(3,6)	39	(4,6)	47	(6,5)	55	(5,8)
8	(2,3)	16	(1,6)	24	(3,5)	32	(4,5)	40	(5,5)	48	(7,4)	56	(6,7)
													64 (8,8)

Let (k_s, k_r) be the m -th candidate pair in the candidate sequence \mathcal{P} . The estimator is

$$(\hat{K}_s, \hat{K}_r) = \min_{\text{lex}} \left\{ m \in \{1, 2, \dots, M^2\} : \hat{T}_n(k_s, k_r) < t_n \right\},$$

where $t_n = n^{-\varepsilon}$ for $\varepsilon \in (0, 0.5)$ is a decaying threshold. Algorithm 2 below summarizes the details of this sequential testing procedure.

Algorithm 2 DiGoF

Require: Adjacency matrix A , significance threshold t_n (default $t_n = n^{-1/5}$), maximum candidate number K_{\max} (default $K_{\max} = \lfloor \sqrt{n/\log n} \rfloor$), where n is the number of nodes

Ensure: Estimated community numbers (\hat{K}_s, \hat{K}_r)

- 1: Generate candidate sequence $\mathcal{P} = [(k_s, k_r)]_{m=1}^M$ with $M = K_{\max}^2$ in lexicographical order
- 2: **for** $m = 1$ to M **do**
- 3: Let $(k_s, k_r) \leftarrow \mathcal{P}(m)$
- 4: Compute $\hat{T}_n(k_s, k_r)$ via Equation (3)
- 5: **if** $\hat{T}_n(k_s, k_r) < t_n$ **then**
- 6: **return** $(\hat{K}_s, \hat{K}_r) = (k_s, k_r)$
- 7: **end if**
- 8: **end for**
- 9: **return** $(\hat{K}_s, \hat{K}_r) = \mathcal{P}(M)$ ▷ If no candidate satisfies $\hat{T}_n < t_n$, return the largest candidate

K_{\max} in Algorithm 2 is set as $\lfloor \sqrt{\frac{n}{\log n}} \rfloor$, where this value is suggested by Assumption 3. The algorithm starts at $(1, 1)$ and sequentially evaluates the test statistic $\hat{T}_n(k_s, k_r)$ for each candidate pair in the lexicographical order. It stops at the first pair (k_s, k_r) where $\hat{T}_n(k_s, k_r) < t_n$ and returns $(\hat{K}_s, \hat{K}_r) = (k_s, k_r)$ as the estimated community numbers.

Remark 3. (Rationale for the lexicographical order). *The lexicographical search order $(k_s, k_r) <_{lex} (k'_s, k'_r)$ is designed to align with the asymptotic behavior of the test statistic \hat{T}_n shown in Theorems 1-2 and ensure computational efficiency:*

- *It prioritizes candidate pairs with minimal total communities $k_s + k_r$. Since underfitted models ($k_s < K_s$ or $k_r < K_r$) yield $\hat{T}_n \xrightarrow{P} \infty$ by Theorem 2, they are quickly rejected. The algorithm only proceeds to higher-complexity candidates when necessary, stopping at the first pair where $\hat{T}_n < t_n$ (likely near the true $K_s + K_r$).*
- *By testing simpler models first (e.g., $(1,1) \rightarrow (1,2) \rightarrow (2,1)$), the algorithm avoids expensive computations for overfitted candidates (e.g., $(5,10)$) if earlier pairs fit the data.*
- *It embodies Occam's razor by favoring lesser parameterizations ($k_s \times k_r$ blocks), reducing the risk of overfitting.*

Remark 4. *It is crucial to emphasize that the sequential search algorithm operates solely based on the established convergence of the upper bound of the test statistic \hat{T}_n to zero under the null hypothesis, without requiring characterization of its lower bound or asymptotic distribution. The algorithm accepts a candidate pair (k_s, k_r) exclusively when \hat{T}_n falls below the decaying threshold t_n —an event guaranteed with high probability under the true model (K_s, K_r) . While characterizing the precise concentration (including lower bounds) or limiting distribution of \hat{T}_n under H_0 remains theoretically valuable, such knowledge is unnecessary for the algorithm's consistency. The divergence of \hat{T}_n to infinity under alternative hypotheses further ensures that underfitted models are rejected with high probability, independently of \hat{T}_n 's lower-tail behavior or limit distribution under H_0 .*

The following theorem guarantees that the sequential procedure achieves joint consistency in recovering the true community numbers under ScBM.

Theorem 3. *Under Assumptions 1-3, let (\hat{K}_s, \hat{K}_r) be obtained from Algorithm 2 with $t_n = n^{-\varepsilon}$ for any $\varepsilon > 0$, we have*

$$\lim_{n \rightarrow \infty} \mathbb{P}((\hat{K}_s, \hat{K}_r) = (K_s, K_r)) = 1.$$

This result establishes that DiGoF correctly identifies both sender and receiver community counts with probability approaching 1 as $n \rightarrow \infty$. The lexicographical search ensures the first acceptable pair coincides with (K_s, K_r) asymptotically.

Remark 5. (Threshold selection). *Though DiGoF enjoys consistency of estimation for any $\varepsilon > 0$ in Theorem 3. Our numerical experiments in Section 5 find that DiGoF is robust for $\varepsilon < 0.5$, with accuracy declining when $\varepsilon \geq 0.65$. This occurs because excessively rapid decay ($\varepsilon \geq 0.5$) makes t_n vulnerable to random fluctuations in \hat{T}_n . Therefore, we recommend $\varepsilon \in (0, 0.5)$ and set default $\varepsilon = 0.2$ for typical n .*

4.2. Ratio-based variant of DiGoF and its estimation consistency

While DiGoF provides consistent estimation under ScBM, its sensitivity to threshold selection may hinder robustness in real-world directed networks with model misspecification. To mitigate this, we propose a ratio-based estimator that identifies the transition point corresponding to the true community structure in the test statistic sequence, leveraging relative changes rather than absolute magnitudes.

For convenience, for each $m \in \{1, 2, \dots, M\}$, here we let $\hat{T}_n(m)$ denote the \hat{T}_n computed for the m -th candidate pair in \mathcal{P} using Equation (3). Define the ratio statistic for the m -th candidate pair as

$$r_m = \left| \frac{\hat{T}_n(m-1)}{\hat{T}_n(m)} \right|, \quad m = 2, 3, \dots, M, \quad (4)$$

where the absolute value addresses potential negative value of \hat{T}_n for the true model (K_s, K_r) .

Theorems 1 and 2 guarantee that under the true model (K_s, K_r) (with lexicographic index m_* in \mathcal{P}), the upper bound of $\hat{T}_n(m_*)$ converges to zero with high probability, while $\hat{T}_n(m_* - 1)$ diverges to infinity under underfitting when $m_* > 1$. Consequently, we shall expect that $r_{m_*} = |\hat{T}_n(m_* - 1)/\hat{T}_n(m_*)|$ is the first significant peak (change point) in the ratio sequence $\{r_m\}_{m=2}^M$. We refer to this method as Ratio-DiGoF (RDiGoF for short), which identifies the first peak in the sequence $\{(m, r_m)\}_{m=2}^M$. The complete RDiGoF algorithm is summarized in Algorithm 3.

Algorithm 3 RDiGoF

Require: Adjacency matrix A , threshold $\tau > 0$ (default $\tau = 10$), maximum candidate number K_{\max} (default $K_{\max} = \lfloor \sqrt{n / \log n} \rfloor$), where n is the number of nodes

Ensure: Estimated community numbers (\hat{K}_s, \hat{K}_r)

- 1: Generate candidate sequence $\mathcal{P} = [(k_s, k_r)]_{m=1}^M$ with $M = K_{\max}^2$ in lexicographical order
- 2: Compute $\hat{T}_n(1)$ for candidate $(1, 1)$ via Equation (3)
- 3: **if** $\hat{T}_n(1) < n^{-1/5}$ **then**
- 4: **return** $(\hat{K}_s, \hat{K}_r) = (1, 1)$
- 5: **end if**
- 6: **for** $m = 2$ to M **do**
- 7: Compute ratio statistic r_m via Equation (4)
- 8: **if** $r_m > \tau$ **then**
- 9: **return** $(\hat{K}_s, \hat{K}_r) = \mathcal{P}(m)$
- 10: **end if**
- 11: **end for**
- 12: **return** $(\hat{K}_s, \hat{K}_r) = \mathcal{P}(M)$ ▷ If no candidate satisfies $r_m > \tau$, return the largest candidate

The following theoretical results establish the estimation consistency of RDiGoF, analogous to Theorems 2 and 3.

Theorem 4. *Under the assumptions of Theorem 3, and assuming additionally that $\delta_n \geq \delta_{\min} > 0$ for all n and that $K_{\max} = \max(K_s, K_r)$ is fixed, then:*

1. *For underfitted models ($m < m_*$): $r_m = O_P(1)$.*

2. For the true model ($m = m_*$): $r_{m_*} \xrightarrow{P} \infty$.

Theorem 5. Under the assumptions of Theorem 4, let (\hat{K}_s, \hat{K}_r) be the output of Algorithm 3. Then there exists a constant $C > 0$ such that if $\tau > C$,

$$\lim_{n \rightarrow \infty} \mathbb{P}((\hat{K}_s, \hat{K}_r) = (K_s, K_r)) = 1.$$

5. Numerical experiments

In this section, we conduct comprehensive numerical studies to evaluate four aspects of our method: (1) convergence behavior of \hat{T}_n under H_0 to verify Theorem 1, (2) behavior characteristics of DiGoF under both correctly specified and underfitted models to verify Theorem 2, (3) estimation accuracy of DiGoF and RDGoF in estimating the numbers of sender and receiver communities across various ScBM parameter settings, and (4) DiGoF's (and RDGoF's) sensitivity to the threshold selection t_n (and τ). Unless specified, we set $\varepsilon = 1/5$ in DiGoF and $\tau = 10$ in RDGoF. Directed networks are generated under ScBM as follows:

- (I) Assign each node to each sender (or receiver) community with equal probability.
- (II) Unless specified, construct the block probability matrix $B \in [0, 1]^{K_s \times K_r}$ as below

$$B(k, l) = \rho \cdot \begin{cases} \alpha + \beta & \text{if } k = l \text{ and } k \leq \min(K_s, K_r) \\ \beta & \text{otherwise} \end{cases}$$

where $\alpha = 0.7$, $\beta = 0.2$, and $\rho \in (0, 1)$ is a sparsity parameter that controls the sparsity of a directed network.

- (III) Generate A via Definition 1 with independent entries

$$A(i, j) \sim \text{Bernoulli}(B(g^s(i), g^r(j))) \quad \text{for } i \neq j, \quad A(i, i) = 0.$$

5.1. Convergence of \hat{T}_n under null hypothesis

We verify Theorem 1 by simulating \hat{T}_n under H_0 : $(K_{s0}, K_{r0}) = (K_s, K_r)$. We set network sizes $n \in \{200, 400, \dots, 2000\}$, $(K_s, K_r) \in \{(1, 2), (2, 2), (2, 3), (2, 4), (3, 4), (3, 5)\}$, and sparsity levels $\rho \in \{0.05, 0.1\}$. For each parameter configuration, we generate 200 independent directed networks and compute the mean \hat{T}_n value. As shown in Figure 1, \hat{T}_n converges to zero as n increases across all configurations, validating Theorem 1. Meanwhile, convergence rates exhibit significant dependence on network sparsity (ρ). For $\rho = 0.05$, \hat{T}_n decays more slowly than under $\rho = 0.1$, reflecting greater variance in the residual matrix under sparser regimes.

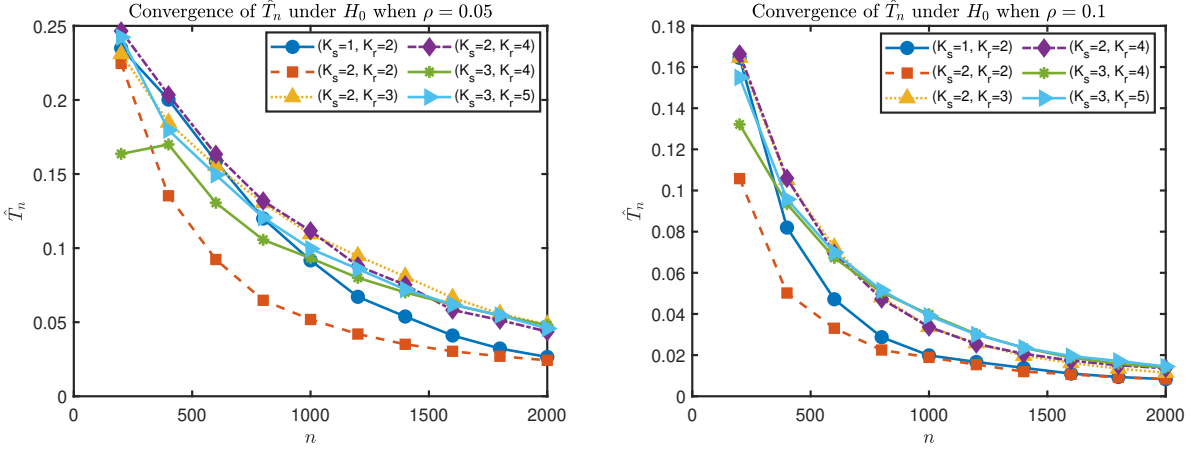


Fig. 1. Behavior of \hat{T}_n under H_0 as network size n increases in different configurations of sender/receiver communities and network sparsity.

5.2. DiGoF's behavior under true and underfitted models

To validate the theoretical properties in Theorems 1 and 2, we quantify DiGoF's acceptance rate under true models and rejection rate under underfitted models. The acceptance rate measures the probability that DiGoF accepts the true community pair $(K_{s0}, K_{r0}) = (K_s, K_r)$ when $\hat{T}_n < t_n$, while the rejection rate captures the probability of $\hat{T}_n \geq t_n$ when either $K_{s0} < K_s$ or $K_{r0} < K_r$. We fix $n = 1000$ and $\rho = 0.1$, with true community structures $(K_s, K_r) \in \{(2, 3), (3, 3), (3, 4)\}$. For each true structure, we evaluate all candidate pairs (K_{s0}, K_{r0}) satisfying $K_{s0} \leq K_s$, $K_{r0} \leq K_r$, and $(K_{s0}, K_{r0}) \neq (K_s, K_r)$. Each configuration undergoes 200 replications. Table 2 summarizes the results, showing 100% acceptance rates for correctly specified models and 100% rejection rates for underfitted models, confirming theoretical predictions across sender-only, receiver-only, and joint underfitting scenarios. This sharp dichotomy between perfect rejection of underfitted models and full acceptance of the true model underscores the statistical discriminative power of the proposed goodness-of-fit test.

5.3. Accuracy of DiGoF and RDiGoF

We evaluate the accuracy of DiGoF and RDiGoF in estimating sender and receiver community numbers under varied parameter settings. We set true community number pairs $(K_s, K_r) \in \{(1, 1), (1, 2), (2, 3), (3, 3), (3, 4), (5, 4)\}$ to maintain $|K_s - K_r| \leq 1$ to make B satisfy Assumption 3. Network sizes range over $n \in \{200, 400, 600, 800, 1000\}$ with sparsity levels $\rho \in \{0.1, 0.2, 0.3, 0.4\}$. Table 3 reports the empirical accuracy $\mathbb{P}((\hat{K}_s, \hat{K}_r) = (K_s, K_r))$ computed over 100 independent replications. The results shown in Table 3 reveal critical performance trends under varying ScBM configurations. For simple structures like $(1, 1)$ and $(1, 2)$, DiGoF achieves perfect accuracy (1.00) across all n and ρ , demonstrating robustness to sparsity when community counts are low. However, for complex structures (e.g., $(2, 3)$, $(3, 4)$, $(5, 4)$), accuracy exhibits a phase transition: at $n = 200$ and low sparsity ($\rho = 0.1$), accuracy drops sharply

Table 2: Rejection rate for different true and hypothesized community pairs.

True (K_s, K_r)	Hypothesized (K_{s0}, K_{r0})	Rejection rate	Underfitting type
(2,3)	(1,1)	1.00	Sender & receiver
	(1,2)	1.00	Sender & receiver
	(1,3)	1.00	Sender only
	(2,1)	1.00	Receiver only
	(2,2)	1.00	Receiver only
	(2,3)	0	–
(3,3)	(1,1)	1.00	Sender & receiver
	(1,2)	1.00	Sender & receiver
	(1,3)	1.00	Sender only
	(2,1)	1.00	Sender & receiver
	(2,2)	1.00	Sender & receiver
	(2,3)	1.00	Sender only
	(3,1)	1.00	Receiver only
	(3,2)	1.00	Receiver only
	(3,3)	0	–
(3,4)	(1,1)	1.00	Sender & receiver
	(1,2)	1.00	Sender & receiver
	(1,3)	1.00	Sender & receiver
	(1,4)	1.00	Sender only
	(2,1)	1.00	Sender & receiver
	(2,2)	1.00	Sender & receiver
	(2,3)	1.00	Sender & receiver
	(2,4)	1.00	Sender only
	(3,1)	1.00	Receiver only
	(3,2)	1.00	Receiver only
	(3,3)	1.00	Receiver only
	(3,4)	0	–

(e.g., 0.00 for (2, 3) and (5, 4)), indicating insufficient signal for detection. As network size n (or sparsity parameter ρ) increases, accuracy improves monotonically. This confirms that larger networks and denser edges enhance community recovery, with DiGoF achieving asymptotic consistency shown in Theorem 3. Furthermore, based on Table 3, RDGoF demonstrates comparable accuracy to DiGoF in most scenarios, particularly as network size or density increases. While it exhibits slight underperformance in very sparse/small settings (e.g., (1,2) at $n = 200, \rho = 0.1$), it matches or marginally exceeds DiGoF in more complex or denser cases (e.g., (5,4) at $n = 600, \rho = 0.2$). Overall, both methods converge rapidly to near-perfect accuracy under sufficient signal.

Table 3: Accuracy of DiGoF and RDGoF under varying sparsity levels ρ for different network sizes n and community number pairs (K_s, K_r) .

(K_s, K_r)	n	DiGoF				RDGoF			
		$\rho = 0.1$	$\rho = 0.2$	$\rho = 0.3$	$\rho = 0.4$	$\rho = 0.1$	$\rho = 0.2$	$\rho = 0.3$	$\rho = 0.4$
(1,1)	200	1.00	1.00	1.00	1.00	1.00	1.00	1.00	1.00
	400	1.00	1.00	1.00	1.00	1.00	1.00	1.00	1.00
	600	1.00	1.00	1.00	1.00	1.00	1.00	1.00	1.00
	800	1.00	1.00	1.00	1.00	1.00	1.00	1.00	1.00
	1000	1.00	1.00	1.00	1.00	1.00	1.00	1.00	1.00
(1,2)	200	1.00	1.00	1.00	1.00	0.65	1.00	1.00	1.00
	400	1.00	1.00	1.00	1.00	1.00	1.00	1.00	1.00
	600	1.00	1.00	1.00	1.00	1.00	1.00	1.00	1.00
	800	1.00	1.00	1.00	1.00	1.00	1.00	1.00	1.00
	1000	1.00	1.00	1.00	1.00	1.00	1.00	1.00	1.00
(2,3)	200	0.10	0.43	0.99	1.00	0.06	0.83	1.00	1.00
	400	0.75	1.00	1.00	1.00	0.94	1.00	1.00	1.00
	600	1.00	1.00	1.00	1.00	1.00	1.00	1.00	1.00
	800	1.00	1.00	1.00	1.00	1.00	1.00	1.00	1.00
	1000	1.00	1.00	1.00	1.00	1.00	1.00	1.00	1.00
(3,3)	200	0.00	0.99	1.00	1.00	0.16	1.00	1.00	1.00
	400	1.00	1.00	1.00	1.00	0.98	1.00	1.00	1.00
	600	1.00	1.00	1.00	1.00	1.00	1.00	1.00	1.00
	800	1.00	1.00	1.00	1.00	1.00	1.00	1.00	1.00
	1000	1.00	1.00	1.00	1.00	1.00	1.00	1.00	1.00
(3,4)	200	0.00	0.00	0.03	0.64	0.06	0.11	0.45	0.83
	400	0.00	0.67	1.00	1.00	0.12	0.82	1.00	1.00
	600	0.01	1.00	1.00	1.00	0.01	1.00	1.00	1.00
	800	0.87	1.00	1.00	1.00	0.93	1.00	1.00	1.00
	1000	1.00	1.00	1.00	1.00	1.00	1.00	1.00	1.00
(5,4)	200	0.00	0.00	0.00	0.00	0.00	0.00	0.03	0.19
	400	0.00	0.00	0.45	1.00	0.00	0.04	0.62	0.99
	600	0.00	0.47	1.00	1.00	0.00	0.61	0.99	1.00
	800	0.00	1.00	1.00	1.00	0.02	0.99	1.00	1.00
	1000	0.01	1.00	1.00	1.00	0.15	1.00	1.00	1.00

5.4. Robustness to threshold choice

We assess DiGoF's sensitivity to the threshold parameter $t_n = n^{-\varepsilon}$ using fixed network sizes $n \in \{600, 1200\}$, true community structure $(K_s, K_r) = (2, 4)$, and sparsity $\rho = 0.5$. The block probability matrix is explicitly defined as:

$$B = \rho \cdot \begin{bmatrix} 0.1 & 0.9 & 0.4 & 0.1 \\ 0.7 & 0.1 & 0.6 & 0.3 \end{bmatrix}.$$

The threshold parameter ε varies from 0.05 to 1.00 in 0.05 increments, yielding 20 distinct thresholds $t_n = n^{-\varepsilon}$. Accuracy is evaluated over 100 independent replications per ε value. The numerical results displayed in Figure 2 demonstrate that DiGoF maintains high accuracy (≥ 0.95) across a broad threshold range $\varepsilon \in (0.05, 0.55]$, with accuracy decline observed only for $\varepsilon \geq 0.65$. This decline aligns with the convergence behavior of the upper bound of \hat{T}_n shown in Figure 1. In detail, for large ε , the threshold t_n decays excessively fast, causing the algorithm to occasionally fail due to the random fluctuations in \hat{T}_n . Though our theoretical analysis in Theorem 3 shows that DiGoF can consistently determine the numbers of sender and receiver communities for any $\varepsilon > 0$, random fluctuations in \hat{T}_n shown in Figure 1 may cause DiGoF to accept underfitted models for large ε . Thus, DiGoF is robust for moderate ε (< 0.5) but exhibits sensitivity at larger values. We recommend $\varepsilon \in (0, 0.5)$ in practice and set the default value of ε as 0.2 for typical n in DiGoF.

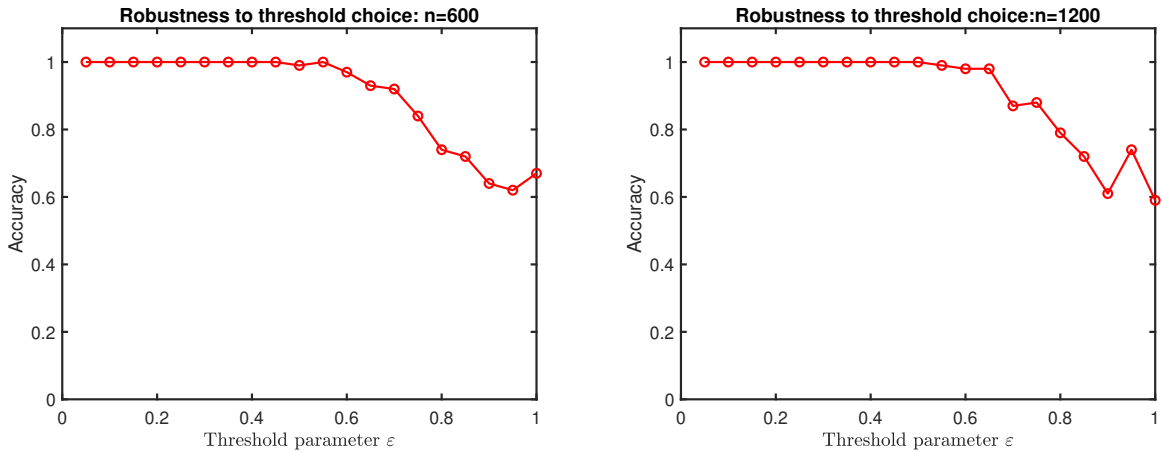


Fig. 2. Accuracy of DiGoF under varying thresholds.

Under the same configuration as in the DiGoF sensitivity analysis, we evaluate the robustness of RDGoF with respect to the threshold parameter τ , varying over the set $\{2, 4, \dots, 20\}$. The results, displayed in Figure 3, indicate that RDGoF achieves nearly perfect accuracy in recovering the true community number pair (K_s, K_r) for all $\tau \geq 4$. This consistency aligns with the theoretical guarantees established in Theorem 5, which requires τ to exceed a certain

positive constant C . In contrast, when $\tau = 2$, the method fails to correctly identify the true community structure. This is expected, as a threshold that is too small may cause the algorithm to mistakenly identify noise fluctuations as significant peaks in the ratio statistic sequence $\{r_m\}_{m=2}^M$, rather than the true transition point corresponding to the true model. Thus, the poor performance at $\tau = 2$ underscores the necessity of choosing a sufficiently large τ to ensure statistical reliability, as required by the theoretical conditions. These findings confirm that RDiGoF is highly robust to the choice of τ within a reasonable range, further supporting its practical utility for asymmetric community numbers estimation in directed networks.

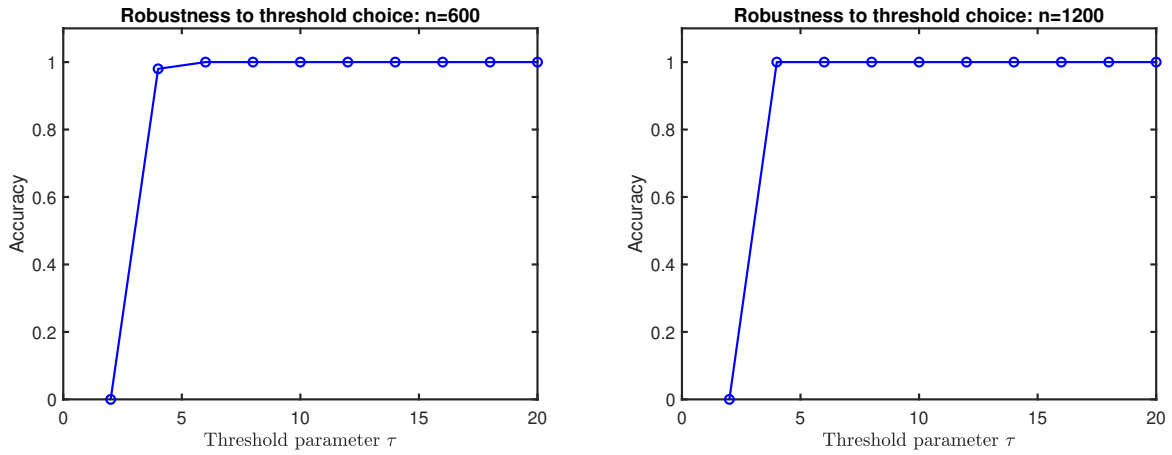


Fig. 3. Accuracy of RDiGoF under varying thresholds.

Remark 6. To investigate the behaviors of $|\hat{T}_n(m)|$ and r_m , we present Figure 4 which displays the sequence of $|\hat{T}_n(m)|$ values (top panels) and corresponding ratio statistics r_m (bottom panels) for candidate community number pairs under the same simulation settings as Figure 2. Results are shown for $n = 600$ (left) and $n = 1200$ (right), with true community structure $(K_s, K_r) = (2, 4)$. The top panels demonstrate the characteristic transition in $|\hat{T}_n(m)|$: underfitted models ($m < m_*$) exhibit large positive values that diverge as predicted by Theorem 2, while at the true model ($m = m_* = 12$), $|\hat{T}_n(m)|$ sharply drops near zero. This transition creates a obvious peak in $\{r_m\}_{m=2}^M$ at m_* (bottom panels), where $r_{m_*} = |\hat{T}_n(m_* - 1)/\hat{T}_n(m_*)|$ becomes substantially larger than 1 ($r_{m_*} > 400$ when $n = 600$ and $r_{m_*} > 1500$ when $n = 1200$). We see that the first significant peak ($r_m > \tau = 10$) in RDiGoF consistently identifies the true community structure across both network sizes.

5.5. Real data examples

In this subsection, we evaluate our method on six real-world directed networks from diverse domains. Basic network statistics are summarized in Table 4, where isolated nodes have been removed and only the largest connected components are retained. All datasets are available at <http://konekt.cc/networks/>.

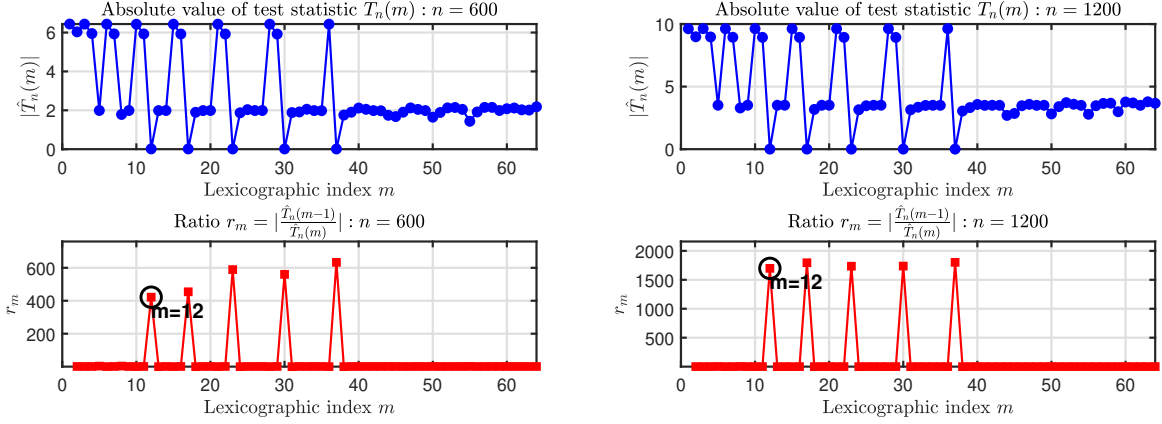


Fig. 4. Absolute value of test statistic sequence $\hat{T}_n(m)$ (top) and ratio statistic r_m (bottom) for lexicographically ordered candidate pairs $1 \leq m \leq 64$ (i.e., $K_{\max} = 8$) at $n = 600$ (left) and $n = 1200$ (right). Black circles indicate the position of the first peak, which is precisely at $m^* = 12$ corresponding to $(K_s, K_r) = (2, 4)$ by Table 1.

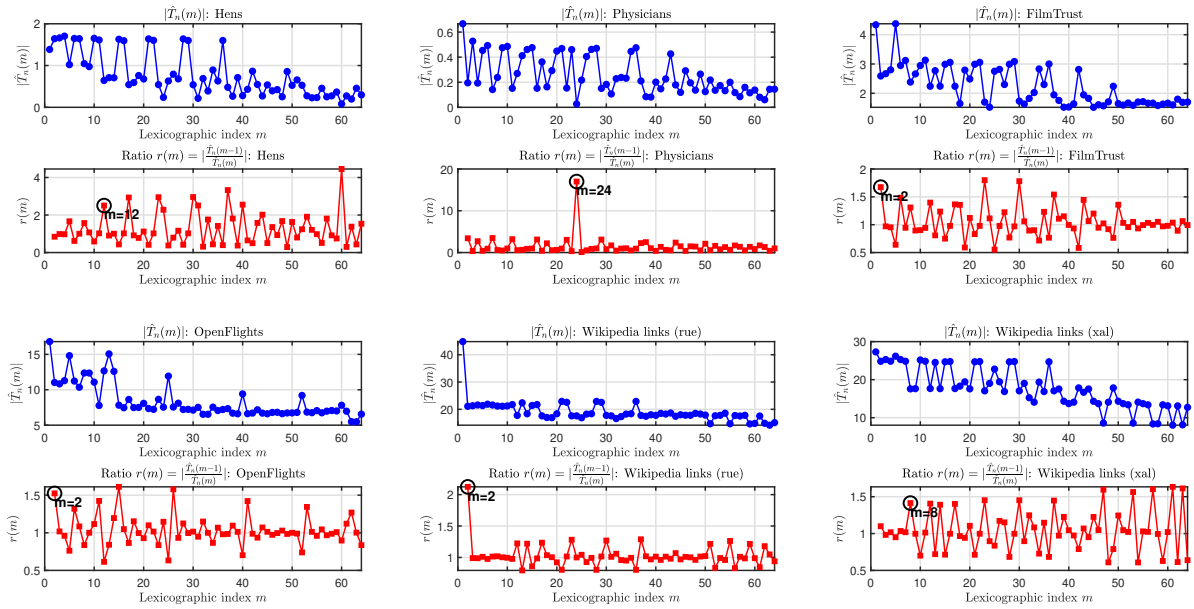


Fig. 5. $|\hat{T}_n(m)|$ and r_m for lexicographically ordered candidate pairs $1 \leq m \leq 64$ (i.e., $K_{\max} = 8$) for real-world directed networks used in this paper. Black circles indicate the first significant peak in r_m identified by RDiGoF.

Table 4: Basic information of real-world directed networks.

Dataset	Source	Node meaning	Directed edge meaning	n	Number of edges	True (K_s, K_r)
Hens	[6]	Hen	Dominance	31	465	Unknown
Physicians	[4]	Physician	Trust	95	458	Unknown
FilmTrust	[7]	User	Trust	347	1254	Unknown
OpenFlights	[27]	Airport	Flight	2868	30404	Unknown
Wikipedia links (rue)	[17]	Wikipedia article in the Rusyn language	Hyperlink	5681	167900	Unknown
Wikipedia links (xal)	[17]	Wikipedia article in the Kalmyk language	Hyperlink	1519	229433	Unknown

Figure 5 displays $|\hat{T}_n(m)|$ and r_m for all real-world directed networks when $K_{\max} = 8$. Unlike simulated directed networks where r_{m_*} exceeds 400 shown in Figure 4, real-world directed networks exhibit substantially smaller ratios:

- $r_m < 2.5$ for FilmTrust, OpenFlights, and both Wikipedia networks.
- $r_m < 5$ for Hens.
- $r_m < 15$ for Physicians.

Consequently, DiGoF fails to select meaningful community numbers even with $\varepsilon \rightarrow 0$, as $|\hat{T}_n(m)|$ never suddenly approaches 0 as shown in the top panels of Figure 5. This phenomenon aligns with observations in real-world undirected networks [19]. Through adjusting the threshold parameter τ , RDGoF overcomes this limitation by identifying the first significant peak in $\{r_m\}_{m=2}^{K_{\max}^2}$. By combining the circled peak points in Figure 5 with the lexicographical order of candidate pairs shown in Table 1, we can obtain the estimated community numbers returned by RDGoF. The results are reported in Table 5. These results demonstrate RDGoF's superior practicality for real-world directed networks, where DiGoF's absolute threshold criterion is inadequate.

Table 5: Estimated community numbers and the corresponding lexicographic index returned by RDGoF for real-world directed networks.

Directed network	(\hat{K}_s, \hat{K}_r)	Lexicographic index m_*
Hens	(2,4)	12
Physicians	(3,5)	24
FilmTrust	(1,2)	2
OpenFlights	(1,2)	2
Wiki (rue)	(1,2)	2
Wiki (xal)	(2,3)	8

6. Conclusion

This paper presents a solution to the critical challenge of jointly estimating sender and receiver community numbers in directed networks under the stochastic co-block model (ScBM). Based on the tail bounds of the largest singular value of a normalized residual matrix, we introduce a novel goodness-of-fit test $\hat{T}_n = \sigma_1(\hat{R}) - 2$, whose asymptotic behavior differs under null and alternative hypotheses. Rigorous theoretical analysis demonstrates that the upper bound

of the proposed test statistic converges to zero with high probability under the null hypothesis with the true sender and receiver community numbers (K_s, K_r), while the test statistic itself diverges to infinity under alternatives where the true model exhibits finer community structures. This sharp dichotomy arises from the asymmetric nature of the residual matrix in directed networks, which precludes the direct application of Tracy-Widom distribution theory established for undirected networks—a gap our work addresses by leveraging singular value tail bounds rather than asymptotic distributions for the estimation of the numbers of sender and receiver communities in directed networks. We then propose a sequential testing algorithm DiGoF to lexicographically seek candidate pairs (k_s, k_r) and stop at the smallest pair where \hat{T}_n falls below a decaying threshold. We further introduce a ratio-based variant algorithm RDiGoF that identifies the transition point in the test statistic sequence to enhance robustness in practical settings. Both algorithms are proven to enjoy consistency in recovering the true (K_s, K_r) within the ScBM framework. Numerical experiments validate the accuracy of both methods across various settings under ScBM, with RDiGoF demonstrating particular advantages in real-world network applications where absolute threshold selection is challenging.

Future research can focus on several interesting questions. First, while we prove the convergence of the upper bound of the test statistic \hat{T}_n to zero under H_0 , establishing whether its lower bound similarly converges to zero would provide a tighter characterization of the statistic’s concentration. Second, even though asymmetry in directed networks causes departures from classical Tracy-Widom limits, investigating whether \hat{T}_n or its scaled variants follow a novel universal distribution remains an open challenge with profound theoretical implications. Further promising directions include extending this framework to degree-corrected ScBM to accommodate degree heterogeneity [30], developing adaptations for multi-layer ScBM [32] or even overlapping community structures [28], and establishing theoretical guarantees under sparser regimes where edge probabilities decay with network size. These extensions would further enhance the method’s applicability to complex real-world directed networks.

CRediT authorship contribution statement

Huan Qing: Conceptualization, Data curation, Formal analysis, Funding acquisition, Methodology, Software, Visualization, Writing – original draft, Writing - review & editing.

Declaration of competing interest

The authors declare no competing interests.

Data availability

Data will be made available on request.

Acknowledgements

Huan Qing was supported by the Scientific Research Foundation of Chongqing University of Technology (Grant No. 2024ZDR003) and the Science and Technology Research Program of Chongqing Municipal Education Commission (Grant No. KJQN202401168).

Appendix A. Proofs for DiGoF

Throughout the appendix, we use the notation introduced in the main text. $\|\cdot\|$ denotes the spectral norm, $\|\cdot\|_F$ the Frobenius norm, and $\sigma_1(\cdot)$ the largest singular value. For two sequences a_n, b_n we write $a_n \ll b_n$ when $a_n = o(b_n)$. The symbols C and c denote generic positive constants whose values may change from line to line.

Proof of Lemma 1. By the statements after Corollary 3.12 in [1], we have the following results for tail bounds of rectangular matrices.

Lemma 2. *Let X be any $n \times m$ random matrix whose entries X_{ij} are independent random variables. Then, for any $0 < \eta \leq 1/2$, there exists a universal constant $c_\eta > 0$ such that for every $t \geq 0$,*

$$\mathbb{P}[\|X\| \geq (1 + \eta)(\varsigma_1 + \varsigma_2) + t] \leq (n \wedge m) \exp\left(-\frac{t^2}{c_\eta \varsigma_*^2}\right),$$

where

$$\varsigma_1 = \max_i \sqrt{\sum_j \mathbb{E}[X_{ij}^2]}, \quad \varsigma_2 = \max_j \sqrt{\sum_i \mathbb{E}[X_{ij}^2]}, \quad \varsigma_* = \max_{ij} \|X_{ij}\|_\infty.$$

For R , under H_0 , $A(i, j)$ are independent Bernoulli($\Omega(i, j)$) variables. Thus, we have

- $\mathbb{E}[R(i, j)] = 0$ for $i \neq j$.
- $\text{Var}(R(i, j)) = \frac{\text{Var}(A(i, j))}{(n-1)\Omega(i, j)(1-\Omega(i, j))} = \frac{\Omega(i, j)(1-\Omega(i, j))}{(n-1)\Omega(i, j)(1-\Omega(i, j))} = \frac{1}{n-1}$.

Thus, let X in Lemma 2 be R , we have $\varsigma_1 = 1$, $\varsigma_2 = 1$, and $\varsigma_* = \frac{1}{\sqrt{\delta(1-\delta)(n-1)}}$. By Lemma 2, we have

$$\mathbb{P}(\|R\| \geq 2(1 + \eta) + t) \leq n \exp\left(-\frac{t^2 \delta(1-\delta)(n-1)}{c_\eta}\right).$$

Let $t = \sqrt{\frac{\gamma \log(n) c_\eta}{\delta(1-\delta)(n-1)}}$ for $\gamma > 2$, we get

$$\mathbb{P}(\|R\| \geq 2(1 + \eta) + t) \leq n \exp\left(\frac{1}{n^{\gamma-1}}\right),$$

which means that with probability at least $1 - o(\frac{1}{n^{\gamma-1}})$, we have

$$\sigma_1(R) - 2 = \|R\| - 2 \leq 2\eta + \sqrt{\frac{\gamma \log(n) c_\eta}{\delta(1-\delta)(n-1)}}. \quad (\text{A.1})$$

Since η is any value in $(0, 1/2]$, δ, C_η , and γ are positive constants, Equation (A.1) means that when Assumption 1 holds, $\mathbb{P}(T_n < \epsilon) \rightarrow 1$ for any $\epsilon > 0$ as $n \rightarrow \infty$. \square

Proof of Theorem 1. First, we bridge the gap between R and \hat{R} . Define $\Delta = \hat{R} - R$. Decompose $\Delta_{ij} = E_1(i, j) + E_2(i, j)$ where:

$$\begin{aligned} E_1(i, j) &= (A(i, j) - \Omega(i, j)) \left(\frac{1}{\sqrt{\hat{\Omega}(i, j)(1 - \hat{\Omega}(i, j))}} - \frac{1}{\sqrt{\Omega(i, j)(1 - \Omega(i, j))}} \right) \frac{1}{\sqrt{n-1}} \\ E_2(i, j) &= \frac{\Omega(i, j) - \hat{\Omega}(i, j)}{\sqrt{(n-1)\hat{\Omega}(i, j)(1 - \hat{\Omega}(i, j))}}. \end{aligned}$$

By mean value theorem and Assumption 1, for ξ_{ij} between $\Omega(i, j)$ and $\hat{\Omega}(i, j)$:

$$\left| \frac{1}{\sqrt{\hat{\Omega}(i, j)(1 - \hat{\Omega}(i, j))}} - \frac{1}{\sqrt{\Omega(i, j)(1 - \Omega(i, j))}} \right| = \frac{1}{2} |2\xi_{ij} - 1| [\xi_{ij}(1 - \xi_{ij})]^{-3/2} |\hat{\Omega}(i, j) - \Omega(i, j)|.$$

Since $\hat{\Omega}(i, j) \in [\delta/2, 1 - \delta/2]$ w.h.p., by continuity, $|2\xi_{ij} - 1| [\xi_{ij}(1 - \xi_{ij})]^{-3/2} \leq C_\delta$ for some $C_\delta > 0$. Thus:

$$|E_1(i, j)| \leq C_\delta |A(i, j) - \Omega(i, j)| \cdot |\hat{\Omega}(i, j) - \Omega(i, j)| \cdot n^{-1/2} \leq C_\delta |\hat{\Omega}(i, j) - \Omega(i, j)| n^{-1/2}$$

since $|A(i, j) - \Omega(i, j)| \leq 1$. Similarly:

$$|E_2(i, j)| \leq \frac{|\Omega(i, j) - \hat{\Omega}(i, j)|}{\sqrt{(n-1) \cdot (\delta/2)(1 - \delta/2)}} = C'_\delta |\hat{\Omega}(i, j) - \Omega(i, j)| n^{-1/2}.$$

Thus, we have

$$|\Delta(i, j)| \leq (C_\delta + C'_\delta) |\hat{\Omega}(i, j) - \Omega(i, j)| n^{-1/2}$$

and

$$\|\Delta\| \leq \|\Delta\|_F \leq C''_\delta n^{-1/2} \|\hat{\Omega} - \Omega\|_F.$$

By Lemma 3, we have

$$\|\hat{\Omega} - \Omega\|_F = O_P\left(K_{\max} \sqrt{\log n}\right).$$

By Assumption 3, we have

$$\|\Delta\| = O_P\left(n^{-1/2} K_{\max} \sqrt{\log n}\right) = o_P(1).$$

By Weyl's inequality, we have

$$|\sigma_1(\hat{R}) - \sigma_1(R)| \leq \|\Delta\| = o_P(1).$$

Thus, we get

$$\sigma_1(\hat{R}) = \sigma_1(R) + o_P(1).$$

By Lemma 1, we know that $\mathbb{P}(T_n < \epsilon) \rightarrow 1$ for any $\epsilon > 0$ as $n \rightarrow \infty$. Therefore, we have

$$\hat{T}_n = \sigma_1(\hat{R}) - 2 = \sigma_1(R) - 2 + o_P(1) = T_n + o_P(1),$$

which gives

$$\mathbb{P}(\hat{T}_n < \epsilon + o_P(1)) \rightarrow 1 \Leftrightarrow \mathbb{P}(\hat{T}_n < \epsilon) \rightarrow 1.$$

□

Proof of Theorem 2. Assume $K_s > K_{s0}$ without loss of generality. By the definition of the community separation parameter δ , there exist sender communities $k_s \neq k_r$ and receiver community l^* such that

$$|B(k_s, l^*) - B(k_r, l^*)| \geq \delta_n.$$

Define node sets:

$$\mathcal{S}_1 = \{i : g^s(i) = k_s\}, \quad s_1 = |\mathcal{S}_1| \geq c_0 n / K_s$$

$$\mathcal{S}_2 = \{i : g^s(i) = k_r\}, \quad s_2 = |\mathcal{S}_2| \geq c_0 n / K_s$$

$$\mathcal{T} = \{j : g^r(j) = l^*\}, \quad t = |\mathcal{T}| \geq c_0 n / K_r.$$

Under H_1 with $K_{s0} < K_s$, by pigeonhole principle, there exists an estimated sender community s_0 such that $\mathcal{S}_1 \cup \mathcal{S}_2 \subseteq \{i : \hat{g}^s(i) = s_0\}$. Meanwhile, since all nodes in \mathcal{T} share the same true receiver label l^* and $K_{r0} \leq K_r$ (possibly $K_{r0} < K_r$), the estimation algorithm forces all nodes in \mathcal{T} (and potentially other nodes) into one estimated

receiver community \hat{t} by pigeonhole principle. Note that when $K_{r0} = K_r$, \hat{g}^r is a consistent receiver community estimator, and the above argument for nodes in \mathcal{T} still holds.

Step 1: Lower bound for expectation difference. Consider the structured residual submatrix $M = (\Omega - \hat{\Omega})(\mathcal{S}_1 \cup \mathcal{S}_2, \mathcal{T})$. For $i \in \mathcal{S}_1$, $\Omega_{ij} = B(k_s, l^*)$, $\hat{\Omega}_{ij} = \hat{B}(s_0, \hat{t})$; for $i \in \mathcal{S}_2$, $\Omega_{ij} = B(k_r, l^*)$, $\hat{\Omega}_{ij} = \hat{B}(s_0, \hat{t})$. Thus, we have

$$M = \begin{bmatrix} (B(k_s, l^*) - \hat{B}(s_0, \hat{t}))\mathbf{1}_{s_1}^\top \\ (B(k_r, l^*) - \hat{B}(s_0, \hat{t}))\mathbf{1}_{s_2}^\top \end{bmatrix} \mathbf{1}_t^\top,$$

where $\mathbf{1}_m^\top$ is a row vector of nodes of length m for any positive integer m . Since M is a rank-1 matrix, its spectral norm satisfies

$$\|M\| = \|\mathbf{v}\mathbf{1}_t^\top\| = \|\mathbf{v}\|_2 \cdot \|\mathbf{1}_t\|_2 = \|\mathbf{v}\|_2 \sqrt{t}$$

where $\mathbf{v} = \begin{bmatrix} (B(k_s, l^*) - \hat{B}(s_0, \hat{t}))\mathbf{1}_{s_1} \\ (B(k_r, l^*) - \hat{B}(s_0, \hat{t}))\mathbf{1}_{s_2} \end{bmatrix}$ is a column vector of length $s_1 + s_2$. Now, we have

$$\|\mathbf{v}\|_2^2 = (B(k_s, l^*) - \hat{B}(s_0, \hat{t}))^2 s_1 + (B(k_r, l^*) - \hat{B}(s_0, \hat{t}))^2 s_2 \geq \min(s_1, s_2) \left[(B(k_s, l^*) - \hat{B}(s_0, \hat{t}))^2 + (B(k_r, l^*) - \hat{B}(s_0, \hat{t}))^2 \right].$$

Using the inequality $a^2 + b^2 \geq (a - b)^2$ for $a \geq 0$ and $b \geq 0$ gives

$$\|\mathbf{v}\|_2^2 \geq \min(s_1, s_2) (B(k_s, l^*) - B(k_r, l^*))^2.$$

Thus, we get

$$\|M\| \geq \sqrt{\min(s_1, s_2) (B(k_s, l^*) - B(k_r, l^*))^2} \cdot \sqrt{t} = \sqrt{\min(s_1, s_2) t} |B(k_s, l^*) - B(k_r, l^*)|.$$

Since $\min(s_1, s_2) \geq c_0 n / K_s$ and $t \geq c_0 n / K_r$ by Assumption 2, we have

$$\|M\| \geq \sqrt{\frac{c_0 n}{K_s} \cdot \frac{c_0 n}{K_r} \delta_n} = c_0 \delta_n \sqrt{\frac{n^2}{K_s K_r}}.$$

Step 2: Control random fluctuation. Let $W = (A - \Omega)(\mathcal{S}_1 \cup \mathcal{S}_2, \mathcal{T})$. We have

$$\sigma_{\text{row}}^2 = \left\| \sum_{i,j} \mathbb{E} [W^{(ij)} (W^{(ij)})^\top] \right\| = \max_i \sum_j \text{Var}(W(i, j)) \leq \frac{t}{4} \leq \frac{n}{4},$$

$$\sigma_{\text{col}}^2 = \left\| \sum_{i,j} \mathbb{E}[(W^{(ij)})^\top W^{(ij)}] \right\| = \max_j \sum_i \text{Var}(W(i, j)) \leq \frac{s_1 + s_2}{4} \leq \frac{n}{2},$$

where $W^{(ij)}$ is the matrix with single entry W_{ij} . Given that $\max(\sigma_{\text{row}}^2, \sigma_{\text{col}}^2) \leq n/2$, by the rectangular case of matrix Bernstein inequality given in Theorem 1.6 of [33], we have

$$\mathbb{P}(\|W\| \geq 3\sqrt{n \log n}) \leq (s_1 + s_2 + t) \exp\left(\frac{-(9n \log n)/2}{n/2 + \sqrt{n \log n}}\right) \leq 3n \cdot n^{-9/2} = 3n^{-7/2} \rightarrow 0,$$

which gives $\|W\| = O_P(\sqrt{n \log n})$.

Step 3: Lower bound for $\sigma_1(\hat{R})$. Since $\hat{\Omega}(i, j) \in [\delta/2, 1 - \delta/2]$ w.h.p. by Lemma 5, we have

$$\sigma_1(\hat{R}) \geq \frac{\|(A - \hat{\Omega})(\mathcal{S}_1 \cup \mathcal{S}_2, \mathcal{T})\|}{\max_{i,j} \sqrt{(n-1)\hat{\Omega}(i, j)(1 - \hat{\Omega}(i, j))}} \geq \frac{\|(A - \hat{\Omega})(\mathcal{S}_1 \cup \mathcal{S}_2, \mathcal{T})\|}{\sqrt{n} \cdot 1/2}$$

as $\hat{\Omega}(i, j)(1 - \hat{\Omega}(i, j)) \leq 1/4$. Now:

$$\|(A - \hat{\Omega})(\mathcal{S}_1 \cup \mathcal{S}_2, \mathcal{T})\| \geq \|M\| - \|W\| \geq c_0 \delta_n \sqrt{\frac{n^2}{K_s K_r}} - O_P(\sqrt{n \log n}).$$

Thus, we have

$$\sigma_1(\hat{R}) \geq \frac{2}{\sqrt{n}} \left(c_0 \delta_n \sqrt{\frac{n^2}{K_s K_r}} - O_P(\sqrt{n \log n}) \right) = 2c_0 \delta_n \sqrt{\frac{n}{K_s K_r}} - O_P\left(\sqrt{\frac{\log n}{n}}\right).$$

By Assumption 3, we have

$$\hat{T}_n = \sigma_1(\hat{R}) - 2 \geq 2c_0 \delta_n \sqrt{\frac{n}{K_s K_r}} - 2 - O_P\left(\sqrt{\frac{\log n}{n}}\right) \geq 2c_0 \delta_n \sqrt{\frac{n}{K_s K_r}} - 2 - o_P(1) \rightarrow \infty,$$

with probability $1 - O(\frac{1}{n^{1/2}})$. □

Proof of Theorem 3. Let $K^* = K_s + K_r$. Define events:

$$\begin{aligned} \mathcal{A} &= \{(\hat{K}_s, \hat{K}_r) \neq (K_s, K_r)\} \\ \mathcal{B} &= \{\exists (k_s, k_r) <_{\text{lex}} (K_s, K_r) : \hat{T}_n(k_s, k_r) < t_n\} \\ C &= \{\hat{T}_n(K_s, K_r) \geq t_n\}. \end{aligned}$$

Then $\mathcal{A} \subseteq \mathcal{B} \cup C$, so $\mathbb{P}(\mathcal{A}) \leq \mathbb{P}(\mathcal{B}) + \mathbb{P}(C)$.

Part 1: $\mathbb{P}(C) \rightarrow 0$. Under $H_0 : (k_s, k_r) = (K_s, K_r)$, by Theorem 1:

$$\hat{T}_n(K_s, K_r) \xrightarrow{P} 0.$$

Since $t_n = Cn^{-\varepsilon} \rightarrow 0$, we get

$$\mathbb{P}(\hat{T}_n(K_s, K_r) \geq t_n) \rightarrow 0.$$

Part 2: $\mathbb{P}(\mathcal{B}) \rightarrow 0$. The underfitting set is:

$$\mathcal{S} = \{(k_s, k_r) \in \mathbb{Z}_+^2 : k_s + k_r \leq K^*, (k_s, k_r) \neq (K_s, K_r)\}$$

with $|\mathcal{S}| \leq (K^*)^2 \leq 4K_{\max}^2$. For each $(k_s, k_r) \in \mathcal{S}$, by Theorem 2:

$$\hat{T}_n(k_s, k_r) \geq c \sqrt{\frac{n\delta_n^2}{K_{\max}^2}}.$$

Since $t_n = n^{-\varepsilon}$ for any $\varepsilon > 0$, by Assumption 3, we have

$$\frac{\sqrt{\frac{n\delta_n^2}{K_{\max}^2}}}{t_n} = \sqrt{\frac{n^{1+2\varepsilon}\delta_n^2}{K_{\max}^2}} \rightarrow \infty.$$

So $\mathbb{P}(\hat{T}_n(k_s, k_r) < t_n) \rightarrow 0$. By Assumption 3 and the proof of Theorem 2, using union bound gives

$$\mathbb{P}(\mathcal{B}) \leq |\mathcal{S}| \max_{(k_s, k_r) \in \mathcal{S}} \mathbb{P}(\hat{T}_n(k_s, k_r) < t_n) = O(K_{\max}^2 \frac{1}{n^{7/2}}) = o(1).$$

Part 3: Conclusion. Since $\mathbb{P}(C) \rightarrow 0$ and $\mathbb{P}(\mathcal{B}) \rightarrow 0$:

$$\mathbb{P}(\mathcal{A}) \leq \mathbb{P}(\mathcal{B}) + \mathbb{P}(C) \rightarrow 0$$

which implies:

$$\lim_{n \rightarrow \infty} \mathbb{P}((\hat{K}_s, \hat{K}_r) = (K_s, K_r)) = 1.$$

□

Appendix A.1. Useful lemmas

Lemma 3. Under the conditions of Theorem 1, the estimated expected adjacency matrix $\hat{\Omega}$ satisfies

$$\|\hat{\Omega} - \Omega\|_F = O_P(K_{\max} \sqrt{\log n}),$$

where m_s (and m_r) is the number of misclustered nodes in the sending (receiving) side.

Proof of Lemma 3. Define the misclustering sets

$$\mathcal{M}^s = \{i : \hat{g}^s(i) \neq g^s(i)\} \text{ with } m_s = |\mathcal{M}^s|,$$

$$\mathcal{M}^r = \{j : \hat{g}^r(j) \neq g^r(j)\} \text{ with } m_r = |\mathcal{M}^r|,$$

The error is decomposed as:

$$\hat{\Omega}(i, j) - \Omega(i, j) = \underbrace{(\hat{B}(k, l) - \bar{B}(k, l))}_{\mathbb{V}_{ij}} + \underbrace{(\bar{B}(k, l) - B(g^s(i), g^r(j)))}_{\mathbb{B}_{ij}},$$

for $k = \hat{g}^s(i)$, $l = \hat{g}^r(j)$, where $\bar{B}(k, l)$ is the conditional expectation:

$$\bar{B}(k, l) = \mathbb{E}[\hat{B}(k, l) | \hat{g}^s, \hat{g}^r] = \frac{1}{|\hat{C}_k^s| \cdot |\hat{C}_l^r|} \sum_{i' \in \hat{C}_k^s} \sum_{j' \in \hat{C}_l^r} B(g^s(i'), g^r(j')).$$

The squared Frobenius norm is:

$$\|\hat{\Omega} - \Omega\|_F^2 = \sum_{i \neq j} (\hat{\Omega}(i, j) - \Omega(i, j))^2 = \underbrace{\sum_{i \neq j} \mathbb{V}_{ij}^2}_{\mathbb{V}} + \underbrace{\sum_{i \neq j} \mathbb{B}_{ij}^2}_{\mathbb{B}} + 2 \underbrace{\sum_{i \neq j} \mathbb{V}_{ij} \mathbb{B}_{ij}}_{\mathbb{C}}.$$

For fixed estimated communities, $\hat{B}(k, l)$ is the average of independent Bernoulli variables. By Lemma 4, we have

$$|\hat{B}(k, l) - \bar{B}(k, l)| = O_P\left(\sqrt{\frac{\log n}{|\hat{C}_k^s||\hat{C}_l^r|}}\right) = O_P\left(\frac{K_{\max} \sqrt{\log n}}{n}\right),$$

which gives

$$\mathbb{V} = \sum_{k, l} \sum_{i \in \hat{C}_k^s} \sum_{j \in \hat{C}_l^r} \mathbb{V}_{ij}^2 = \sum_{k, l} |\hat{C}_k^s| |\hat{C}_l^r| \cdot O_P\left(\frac{K_{\max}^2 \log n}{n^2}\right) = O_P(K_{\max}^2 \log n).$$

The bias term $B_{ij} = \bar{B}(k, l) - B(g^s(i), g^r(j))$ is bounded by considering node misclustering:

$$|B_{ij}| \leq \frac{1}{|\hat{C}_k^s \cap \hat{C}_l^r|} \sum_{i' \in \hat{C}_k^s} \sum_{j' \in \hat{C}_l^r} |B(g^s(i'), g^r(j')) - B(g^s(i), g^r(j))|.$$

Define:

$$\begin{aligned} \mathcal{G}_k^s &= \{i' \in \hat{C}_k^s : g^s(i') = k\}, \quad \mathcal{B}_k^s = \hat{C}_k^s \setminus \mathcal{G}_k^s, \quad |\mathcal{B}_k^s| \leq m_s, \\ \mathcal{G}_l^r &= \{j' \in \hat{C}_l^r : g^r(j') = l\}, \quad \mathcal{B}_l^r = \hat{C}_l^r \setminus \mathcal{G}_l^r, \quad |\mathcal{B}_l^r| \leq m_r. \end{aligned}$$

Then:

$$|B_{ij}| \leq \frac{|\mathcal{B}_k^s| \cdot |\hat{C}_l^r| + |\mathcal{B}_l^r| \cdot |\hat{C}_k^s|}{|\hat{C}_k^s \cap \hat{C}_l^r|} \leq \frac{m_s}{|\hat{C}_k^s|} + \frac{m_r}{|\hat{C}_l^r|} \leq \frac{K_{\max}}{c_0 n} (m_s + m_r).$$

The sum \mathbb{B} is split by clustering status:

$$\mathbb{B} = \sum_{\substack{i \notin \mathcal{M}^s \\ j \notin \mathcal{M}^r}} \mathbb{B}_{ij}^2 + \sum_{\substack{i \in \mathcal{M}^s \text{ or } j \in \mathcal{M}^r}} \mathbb{B}_{ij}^2.$$

For correctly clustered nodes ($i \notin \mathcal{M}^s, j \notin \mathcal{M}^r$):

$$|\mathbb{B}_{ij}| \leq \frac{K_{\max}}{c_0 n} (m_s + m_r) \implies \sum_{\substack{i \notin \mathcal{M}^s \\ j \notin \mathcal{M}^r}} \mathbb{B}_{ij}^2 \leq \left(\frac{K_{\max}}{c_0 n} (m_s + m_r) \right)^2 \cdot n^2 = O_P \left(K_{\max}^2 (m_s + m_r)^2 \right).$$

For misclustered nodes (at least one of i or j misclustered), since $|\mathbb{B}_{ij}| \leq 1$, we have

$$\sum_{i \in \mathcal{M}^s \text{ or } j \in \mathcal{M}^r} \mathbb{B}_{ij}^2 \leq n(m_s + m_r).$$

Thus, we get

$$\mathbb{B} = O_P \left(K_{\max}^2 (m_s + m_r)^2 + n(m_s + m_r) \right).$$

By the Cauchy-Schwarz inequality:

$$|\mathbb{C}| \leq 2 \sqrt{\mathbb{V}} \sqrt{\mathbb{B}} = 2 \sqrt{O_P(K_{\max}^2 \log n)} \cdot \sqrt{O_P \left(K_{\max}^2 (m_s + m_r)^2 + n(m_s + m_r) \right)}.$$

Given that \hat{g}^s and \hat{g}^r are consistent community estimators under the null hypothesis H_0 , we have $\mathbb{P}(m_s = 0) \rightarrow 1$

and $\mathbb{P}(m_r = 0) \rightarrow 1$. Thus, we have

$$\|\hat{\Omega} - \Omega\|_F = O_P\left(K_{\max} \sqrt{\log n}\right).$$

□

Lemma 4. *Under Assumption 1, for any estimated sender community s_0 and receiver community \hat{t} with sizes $n_s = |\{i : \hat{g}^s(i) = s_0\}|$ and $n_t = |\{j : \hat{g}^r(j) = \hat{t}\}|$, the estimated block probability $\hat{B}(s_0, \hat{t})$ satisfies:*

$$|\hat{B}(s_0, \hat{t}) - \mathbb{E}[\hat{B}(s_0, \hat{t})]| \leq \sqrt{\frac{3 \log n}{n_s n_t}}$$

with probability at least $1 - O(n^{-3})$.

Proof of Lemma 4. The estimated block probability is defined as

$$\hat{B}(s_0, \hat{t}) = \frac{1}{n_s n_t} \sum_{i \in \hat{C}_{s_0}^s} \sum_{j \in \hat{C}_{\hat{t}}^r} A(i, j),$$

where $\hat{C}_{s_0}^s = \{i : \hat{g}^s(i) = s_0\}$ and $\hat{C}_{\hat{t}}^r = \{j : \hat{g}^r(j) = \hat{t}\}$. Conditional on the estimated communities \hat{g}^s and \hat{g}^r , the random variables $\{A(i, j)\}_{i \in \hat{C}_{s_0}^s, j \in \hat{C}_{\hat{t}}^r}$ are independent Bernoulli trials with success probabilities $p_{ij} = B(g^s(i), g^r(j)) \in [\delta, 1 - \delta]$ by Assumption 1. Define the centered variables:

$$X_{ij} = A(i, j) - p_{ij}, \quad \text{for } i \in \hat{C}_{s_0}^s, j \in \hat{C}_{\hat{t}}^r.$$

These satisfy $\mathbb{E}[X_{ij} | \hat{g}^s, \hat{g}^r] = 0$, $|X_{ij}| \leq 1$, and $\text{Var}(X_{ij} | \hat{g}^s, \hat{g}^r) = p_{ij}(1 - p_{ij}) \leq \frac{1}{4}$. Consider the sum

$$S = \sum_{i \in \hat{C}_{s_0}^s} \sum_{j \in \hat{C}_{\hat{t}}^r} X_{ij}.$$

The variance of S is bounded by

$$V = \text{Var}(S | \hat{g}^s, \hat{g}^r) \leq \sum_{i,j} \frac{1}{4} = \frac{n_s n_t}{4}.$$

For any $v > 0$, applying Bernstein's inequality [33] to S gives

$$\mathbb{P}(|S| \geq v | \hat{g}^s, \hat{g}^r) \leq 2 \exp\left(-\frac{v^2/2}{V + v/3}\right).$$

Substitute $v = \sqrt{3n_s n_t \log n}$ and $V \leq \frac{n_s n_t}{4}$:

$$\mathbb{P}(|S| \geq \sqrt{3n_s n_t \log n} \mid \hat{g}^s, \hat{g}^r) \leq 2 \exp\left(-\frac{3n_s n_t \log n/2}{\frac{n_s n_t}{4} + \frac{\sqrt{3n_s n_t \log n}}{3}}\right).$$

For large n , $\sqrt{3n_s n_t \log n}/3 \leq n_s n_t/4$ since $n_s n_t \gg \sqrt{n_s n_t \log n}$. Thus, we have

$$\frac{3n_s n_t \log n/2}{n_s n_t/2} = 3 \log n, \quad \text{so} \quad \mathbb{P}(|S| \geq \sqrt{3n_s n_t \log n} \mid \hat{g}^s, \hat{g}^r) \leq 2 \exp(-3 \log n) = 2n^{-3}.$$

Finally, with probability at least $1 - O(n^{-3})$, we have

$$|\hat{B}(s_0, \hat{t}) - \mathbb{E}[\hat{B}(s_0, \hat{t}) \mid \hat{g}^s, \hat{g}^r]| = \frac{|S|}{n_s n_t} \leq \sqrt{\frac{3 \log n}{n_s n_t}}.$$

□

Lemma 5. *Under Assumptions 1-3, and under the alternative hypothesis ($K_{s0} < K_s$ or $K_{r0} < K_r$), the estimated probability matrix entries satisfy*

$$\hat{\Omega}(i, j) \in [\delta/2, 1 - \delta/2] \quad \text{for all } i, j$$

with probability at least $1 - o(n^{-1})$.

Proof of Lemma 5. Recall that for any i, j , $\hat{\Omega}(i, j) = \hat{B}(k, l)$ where $k = \hat{g}^s(i)$, $l = \hat{g}^r(j)$. We prove $\hat{B}(k, l) \in [\delta/2, 1 - \delta/2]$ uniformly over all blocks k, l . The conditional expectation

$$\bar{B}(k, l) = \mathbb{E}[\hat{B}(k, l) \mid \hat{g}^s, \hat{g}^r] = \frac{1}{|\hat{C}_k^s| |\hat{C}_l^r|} \sum_{i' \in \hat{C}_k^s} \sum_{j' \in \hat{C}_l^r} B(g^s(i'), g^r(j'))$$

is a convex combination of $B(\cdot, \cdot) \in [\delta, 1 - \delta]$ (Assumption 1). Thus,

$$\bar{B}(k, l) \in [\delta, 1 - \delta] \quad \forall k, l.$$

By Lemma 4, for any fixed (k, l) , with probability at least $1 - O(\frac{1}{n^3})$, we have

$$|\hat{B}(k, l) - \bar{B}(k, l)| \leq \sqrt{\frac{3 \log n}{n_k n_l}},$$

where $n_k = |\hat{C}_k^s|$, $n_l = |\hat{C}_l^r|$. Under H_1 ($K_{s0} \leq K_s$, $K_{r0} \leq K_r$), the pigeonhole principle implies each estimated

community contains at least one true community. By Assumption 2, we have

$$n_k \geq \min_{k'} |\{i : g^s(i) = k'\}| \geq c_0 \frac{n}{K_s} \geq c_0 \frac{n}{K_{\max}}, \quad n_l \geq c_0 \frac{n}{K_{\max}}.$$

Thus, $n_k n_l \geq (c_0 n / K_{\max})^2$, which gives

$$\sqrt{\frac{3 \log n}{n_k n_l}} \leq \frac{K_{\max} \sqrt{3 \log n}}{c_0 n}.$$

By Assumption 3, we have

$$\frac{K_{\max} \sqrt{\log n}}{n} = \frac{1}{\sqrt{n}} \sqrt{\frac{K_{\max}^2 \log n}{n}} = o\left(\frac{1}{\sqrt{n}}\right).$$

For large n , $\frac{1}{\sqrt{n}} \ll \delta/2$. Thus, with probability at least $1 - O(n^{-3})$, for per block, we have

$$\hat{B}(k, l) \in \left[\bar{B}(k, l) - \frac{\delta}{2}, \bar{B}(k, l) + \frac{\delta}{2} \right] \subseteq \left[\frac{\delta}{2}, 1 - \frac{\delta}{2} \right].$$

There are $\leq K_{s0} K_{r0} \leq K_{\max}^2$ blocks. Then, by Assumption 3, the union bound gives

$$\mathbb{P}\left(\bigcup_{k,l} \left\{ |\hat{B}(k, l) - \bar{B}(k, l)| > \frac{\delta}{2} \right\}\right) = O(K_{\max}^2 n^{-3}) \ll O\left(\frac{n}{\log n} n^{-3}\right) = O\left(\frac{n^{-2}}{\log n}\right).$$

Thus, with probability at least $1 - o(n^{-1})$, we have all $\hat{\Omega}(i, j) \in [\delta/2, 1 - \delta/2]$. \square

Appendix B. Proofs for RDiGoF

This section provides the detailed proofs of Theorems 4 and 5. We begin by establishing several useful lemmas.

Lemma 6. *Under the assumptions of Theorem 4, we have*

1. $\hat{T}_n(m) \geq -2$.
2. *For underfitted models ($m < m_*$): For any $c > 0$, $\lim_{n \rightarrow \infty} \mathbb{P}(\hat{T}_n(m) > c) = 1$.*
3. *For the true model ($m = m_*$): $\lim_{n \rightarrow \infty} \mathbb{P}(|\hat{T}_n(m_*)| \leq 2) = 1$.*

Proof of Lemma 6. Since singular values are non-negative, $\sigma_1(\hat{R}) \geq 0$, so $\hat{T}_n(m) = \sigma_1(\hat{R}) - 2 \geq -2$.

Let $d_n = \frac{\delta_n \sqrt{n}}{K_{\max}}$. From the proof of Theorem 2, there exists $c_1 > 0$ such that $\hat{T}_n(m) \geq c_1 d_n - 2 - o_P(1)$. Since $K_{\max} = O(1)$ and $\delta_n \geq \delta_{\min}$, $d_n = \delta_n \sqrt{n} / K_{\max} \geq \delta_{\min} \sqrt{n} / K_{\max} = O(\sqrt{n}) \rightarrow \infty$. Then there exists N such that for $n > N$, $\mathbb{P}(\hat{T}_n(m) > c) = 1$ for any $c > 0$. Hence, $\lim_{n \rightarrow \infty} \mathbb{P}(\hat{T}_n(m) > c) = 1$.

By Theorem 1, for any $\epsilon > 0$, $\lim_{n \rightarrow \infty} \mathbb{P}(\hat{T}_n(m_*) < \epsilon) = 1$. Taking $\epsilon = 2$, we have $\mathbb{P}(\hat{T}_n(m_*) < 2) \rightarrow 1$. Since $\hat{T}_n(m_*) \geq -2$ always holds, it follows that $\mathbb{P}(|\hat{T}_n(m_*)| \leq 2) \rightarrow 1$. \square

Lemma 7. *Under the assumptions of Theorem 4, there exists a constant $C > 0$ such that for all $m < m_*$, we have*

$$\lim_{n \rightarrow \infty} \mathbb{P}(r_m \leq C) = 1.$$

Proof of Lemma 7. From the proof of Theorem 2,

$$\hat{T}_n(m) \geq c_1 d_n - 2 - o_P(1).$$

Take $c_{\text{low}} = c_1/2$. Since $d_n \rightarrow \infty$, there exists N such that for $n > N$, $c_1 d_n - 2 - o_P(1) > c_{\text{low}} d_n + 1$. Hence, we have $\lim_{n \rightarrow \infty} \mathbb{P}(\hat{T}_n(m) \geq c_{\text{low}} d_n) = 1$.

By Lemma 5, with probability at least $1 - o(n^{-1})$, $\hat{\Omega}(i, j) \in [\delta/2, 1 - \delta/2]$ for all i, j . Therefore, we have

$$\hat{\Omega}(i, j)(1 - \hat{\Omega}(i, j)) \geq \gamma_\delta = (\delta/2)(1 - \delta/2) \geq \frac{\delta(1 - \delta)}{4}.$$

Let $\mu = \delta(1 - \delta)/4$. Then for $i \neq j$,

$$|\hat{R}(i, j)| = \frac{|A(i, j) - \hat{\Omega}(i, j)|}{\sqrt{(n-1)\hat{\Omega}(i, j)(1 - \hat{\Omega}(i, j))}} \leq \frac{|A(i, j) - \hat{\Omega}(i, j)|}{\sqrt{(n-1)\mu}}.$$

Thus, the spectral norm satisfies

$$\|\hat{R}\| \leq \frac{1}{\sqrt{(n-1)\mu}} \|A - \hat{\Omega}\|.$$

Now, we bound $\|A - \hat{\Omega}\|$ by decomposing it as $A - \hat{\Omega} = (A - \Omega) + (\Omega - \hat{\Omega})$. Since $A - \Omega$ has independent mean-zero entries with variance at most $1/4$, by Bernstein's inequality, we have $\|A - \Omega\| = O_P(\sqrt{n})$. Since entries of Ω and $\hat{\Omega}$ are in $[0, 1]$, we have $\|\Omega - \hat{\Omega}\|_F \leq n$, hence $\|\Omega - \hat{\Omega}\| \leq \|\Omega - \hat{\Omega}\|_F \leq n$. Therefore, we have

$$\|A - \hat{\Omega}\| \leq \|A - \Omega\| + \|\Omega - \hat{\Omega}\| = O_P(\sqrt{n}) + n = O(n),$$

which gives

$$\hat{T}_n(m) = \|\hat{R}\| - 2 \leq \frac{O(n)}{\sqrt{(n-1)\mu}} - 2 = O(\sqrt{n}).$$

Since $\delta_n \geq \delta_{\min} > 0$ and K_{\max} is bounded, we have $d_n = \delta_n \sqrt{n}/K_{\max} = O(\sqrt{n})$. Therefore, there exists a constant

$C_{\text{upp}} > 0$ such that

$$\lim_{n \rightarrow \infty} \mathbb{P}(\hat{T}_n(m) \leq C_{\text{upp}} d_n) = 1.$$

Therefore, we get

$$r_m = \frac{\hat{T}_n(m-1)}{\hat{T}_n(m)} \leq \frac{C_{\text{upp}} d_n}{c_{\text{low}} d_n} = \frac{C_{\text{upp}}}{c_{\text{low}}} = C.$$

□

Proof of Theorem 4. For underfitted models ($m < m_*$): By Lemma 7, $r_m \leq C$ with high probability, so $r_m = O_P(1)$.

For the true model ($m = m_*$): Let $X = \hat{T}_n(m_* - 1)$ and $Y = \hat{T}_n(m_*)$. By Lemma 6, we have

$$\lim_{n \rightarrow \infty} \mathbb{P}(X > 2c) = 1 \quad \text{for any } c > 0, \quad \text{and} \quad \lim_{n \rightarrow \infty} \mathbb{P}(|Y| \leq 2) = 1.$$

Fix $c > 0$. Then, we get

$$\mathbb{P}(X > 2c) \rightarrow 1, \quad \mathbb{P}(|Y| \leq 2) \rightarrow 1.$$

Thus, the ratio statistic $r_{m_*} = \left| \frac{X}{Y} \right| \geq \frac{X}{2} > c$ with high probability. Therefore, for any $c > 0$, we have

$$\mathbb{P}(r_{m_*} > c) \rightarrow 1.$$

Hence, we have $r_{m_*} \xrightarrow{P} \infty$.

□

Proof of Theorem 5. Fix $\tau > C$, where C is the one in Lemma 7. Define two events:

$$E_1 = \{r_{m_*} > 2\tau\}, \quad E_2 = \{r_m \leq \tau \text{ for all } m = 2, \dots, m_* - 1\}.$$

By Theorem 4, for any $\tau' > 0$, $\mathbb{P}(r_{m_*} > \tau') \rightarrow 1$. In particular, take $\tau' = 2\tau$, then $\mathbb{P}(E_1) \rightarrow 1$. By Lemma 7, for each $m < m_*$, $\mathbb{P}(r_m > \tau) \rightarrow 0$. Since $m_* \leq K_{\max}^2$ and K_{\max} is fixed, the number of terms is finite. Thus, by the union bound, we get

$$\mathbb{P}(E_2^c) \leq \sum_{m=2}^{m_*-1} \mathbb{P}(r_m > \tau) \rightarrow 0.$$

Hence, $\mathbb{P}(E_2) \rightarrow 1$. On $E_1 \cap E_2$, we have $r_{m_*} > 2\tau > \tau$ and for all $m < m_*$, $r_m \leq \tau < r_{m_*}$, so r_{m_*} is the first value greater than τ and is the maximum up to m_* . Therefore, the RDGoF algorithm sets $\hat{m}_* = m_*$, where \hat{m}_* is the first m

satisfying $r_m > \tau$ in the RDiGoF algorithm. Thus, we have

$$\mathbb{P}(\hat{m}_* = m_*) \geq \mathbb{P}(E_1 \cap E_2) \rightarrow 1,$$

which implies $\lim_{n \rightarrow \infty} \mathbb{P}((\hat{K}_s, \hat{K}_r) = (K_s, K_r)) = 1$. \square

References

- [1] Bandeira, A.S., van Handel, R., 2016. Sharp nonasymptotic bounds on the norm of random matrices with independent entries. *Annals of Probability* 44, 2479 – 2506.
- [2] Bickel, P.J., Sarkar, P., 2016. Hypothesis testing for automated community detection in networks. *Journal of the Royal Statistical Society Series B: Statistical Methodology* 78, 253–273.
- [3] Chen, K., Lei, J., 2018. Network cross-validation for determining the number of communities in network data. *Journal of the American Statistical Association* 113, 241–251.
- [4] Coleman, J., Katz, E., Menzel, H., 1957. The diffusion of an innovation among physicians. *Sociometry* 20, 253–270.
- [5] Dong, Z., Wang, S., Liu, Q., 2020. Spectral based hypothesis testing for community detection in complex networks. *Information Sciences* 512, 1360–1371.
- [6] Guhl, A.M., 1953. Social behavior of the domestic fowl. .
- [7] Guo, G., Zhang, J., Yorke-Smith, N., 2016. A novel evidence-based bayesian similarity measure for recommender systems. *ACM Transactions on the Web (TWEB)* 10, 1–30.
- [8] Guo, X., Qiu, Y., Zhang, H., Chang, X., 2023. Randomized spectral co-clustering for large-scale directed networks. *Journal of Machine Learning Research* 24, 1–68.
- [9] Holland, P.W., Laskey, K.B., Leinhardt, S., 1983. Stochastic blockmodels: First steps. *Social Networks* 5, 109–137.
- [10] Hu, J., Qin, H., Yan, T., Zhao, Y., 2020. Corrected bayesian information criterion for stochastic block models. *Journal of the American Statistical Association* 115, 1771–1783.
- [11] Hu, J., Zhang, J., Qin, H., Yan, T., Zhu, J., 2021. Using maximum entry-wise deviation to test the goodness of fit for stochastic block models. *Journal of the American Statistical Association* 116, 1373–1382.
- [12] Hwang, N., Xu, J., Chatterjee, S., Bhattacharyya, S., 2024. On the estimation of the number of communities for sparse networks. *Journal of the American Statistical Association* 119, 1895–1910.
- [13] Ji, P., Jin, J., 2016. Coauthorship and citation networks for statisticians. *Annals of Applied Statistics* 10, 1779 – 1812.
- [14] Ji, P., Jin, J., Ke, Z.T., Li, W., 2022. Co-citation and co-authorship networks of statisticians. *Journal of Business & Economic Statistics* 40, 469–485.
- [15] Jin, J., Ke, Z.T., Luo, S., Wang, M., 2023. Optimal estimation of the number of network communities. *Journal of the American Statistical Association* 118, 2101–2116.
- [16] Karrer, B., Newman, M.E., 2011. Stochastic blockmodels and community structure in networks. *Physical Review E—Statistical, Nonlinear, and Soft Matter Physics* 83, 016107.
- [17] Kunegis, J., 2013. Konect: the koblenz network collection, in: *Proceedings of the 22nd International Conference on World Wide Web*, pp. 1343–1350.
- [18] Le, C.M., Levina, E., 2022. Estimating the number of communities by spectral methods. *Electronic Journal of Statistics* 16, 3315 – 3342.

- [19] Lei, J., 2016. A goodness-of-fit test for stochastic block models. *Annals of Statistics* 44, 401–424.
- [20] Lei, J., Rinaldo, A., 2015. Consistency of spectral clustering in stochastic block models. *Annals of Statistics* 43, 215–237.
- [21] Leicht, E.A., Newman, M.E., 2008. Community structure in directed networks. *Physical Review Letters* 100, 118703.
- [22] Li, B., Yang, Y., 2022. Undirected and directed network analysis of the Chinese stock market. *Computational Economics* 60, 1155–1173.
- [23] Li, T., Levina, E., Zhu, J., 2020. Network cross-validation by edge sampling. *Biometrika* 107, 257–276.
- [24] Ma, S., Su, L., Zhang, Y., 2021. Determining the number of communities in degree-corrected stochastic block models. *Journal of Machine Learning Research* 22, 1–63.
- [25] Malliaros, F.D., Vazirgiannis, M., 2013. Clustering and community detection in directed networks: A survey. *Physics Reports* 533, 95–142.
- [26] McDaid, A.F., Murphy, T.B., Friel, N., Hurley, N.J., 2013. Improved bayesian inference for the stochastic block model with application to large networks. *Computational Statistics & Data Analysis* 60, 12–31.
- [27] Opsahl, T., Agneessens, F., Skvoretz, J., 2010. Node centrality in weighted networks: Generalizing degree and shortest paths. *Social Networks* 32, 245–251.
- [28] Qing, H., 2025. Discovering overlapping communities in multi-layer directed networks. *Chaos, Solitons & Fractals* 194, 116175.
- [29] Qing, H., Wang, J., 2023. Community detection for weighted bipartite networks. *Knowledge-Based Systems* 274, 110643.
- [30] Rohe, K., Qin, T., Yu, B., 2016. Co-clustering directed graphs to discover asymmetries and directional communities. *Proceedings of the National Academy of Sciences* 113, 12679–12684.
- [31] Saldana, D.F., Yu, Y., Feng, Y., 2017. How many communities are there? *Journal of Computational and Graphical Statistics* 26, 171–181.
- [32] Su, W., Guo, X., Chang, X., Yang, Y., 2024. Spectral co-clustering in multi-layer directed networks. *Computational Statistics & Data Analysis* 198, 107987.
- [33] Tropp, J.A., 2012. User-friendly tail bounds for sums of random matrices. *Foundations of Computational Mathematics* 12, 389–434.
- [34] Wang, Y.X.R., Bickel, P.J., 2017. Likelihood-based model selection for stochastic block models. *Annals of Statistics* 45, 500 – 528.
- [35] Wang, Z., Liang, Y., Ji, P., 2020. Spectral algorithms for community detection in directed networks. *Journal of Machine Learning Research* 21, 1–45.
- [36] Wu, Q., Hu, J., 2024a. A spectral based goodness-of-fit test for stochastic block models. *Statistics & Probability Letters* 209, 110104.
- [37] Wu, Q., Hu, J., 2024b. Two-sample test of stochastic block models. *Computational Statistics & Data Analysis* 192, 107903.
- [38] Zhang, J., Wang, J., 2022. Identifiability and parameter estimation of the overlapped stochastic co-block model. *Statistics and Computing* 32, 57.
- [39] Zhou, Z., Amini, A.A., 2019. Analysis of spectral clustering algorithms for community detection: the general bipartite setting. *Journal of Machine Learning Research* 20, 1–47.
- [40] Zhou, Z., Amini, A.A., 2020. Optimal bipartite network clustering. *Journal of Machine Learning Research* 21, 1–68.